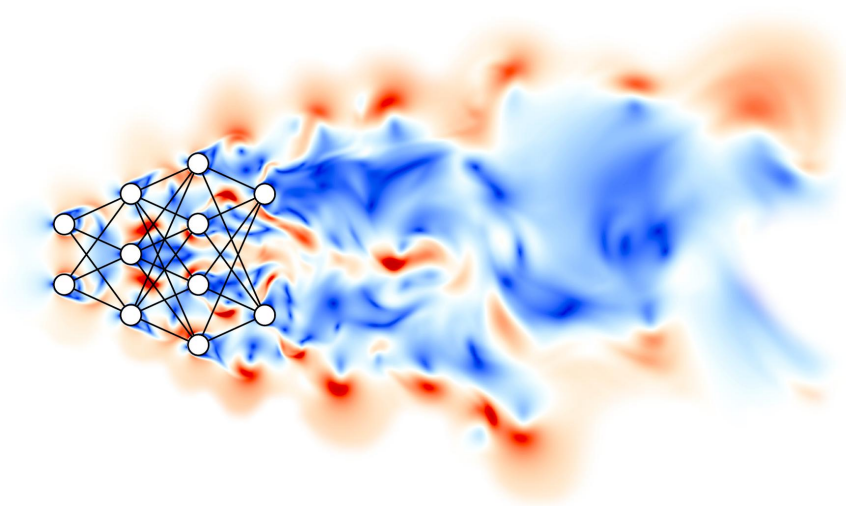


# Improving turbulence control through explainable deep learning

Ricardo Vinuesa<sup>1,2</sup>



<sup>1</sup>FLOW, KTH Engineering Mechanics, Stockholm, Sweden.

<sup>2</sup>Swedish e-Science Research Centre (SeRC), Stockholm, Sweden.



# The Sustainable Development Goals (SDGs)



- **2030 Agenda for Sustainable Development adopted by all United Nations Member States in 2015**
- Shared blueprint for peace and prosperity for people and the planet
- Recognize that **ending poverty and other deprivations must go hand-in-hand** with strategies that improve health and education, reduce inequality, and spur economic growth – all while tackling **climate change** and working to **preserve our oceans and forests**
- **17 different** Sustainable Development Goals (SDGs); **169** targets



# Motivation

- We want to answer the question: “Is there published evidence of **AI acting as an enabler or an inhibitor for each of the SDG targets?**”



Vinuesa et al., Nature Communications 11, 233 (2020)



# Motivation

- We want to answer the question: “Is there published evidence of **AI acting as an enabler or an inhibitor for each of the SDG targets?**”
- We needed to assemble a **multi-disciplinary team** spanning the wide range of required areas of knowledge.



Vinuesa et al., Nature Communications **11**, 233 (2020)



# Dividing the 17 SDGs into 3 main pillars

– We divided the 17 SDGs into 3 main categories (Stockholm Resilience Center, 2017; United Nations, 2019): **Society, Economy, and Environment.**

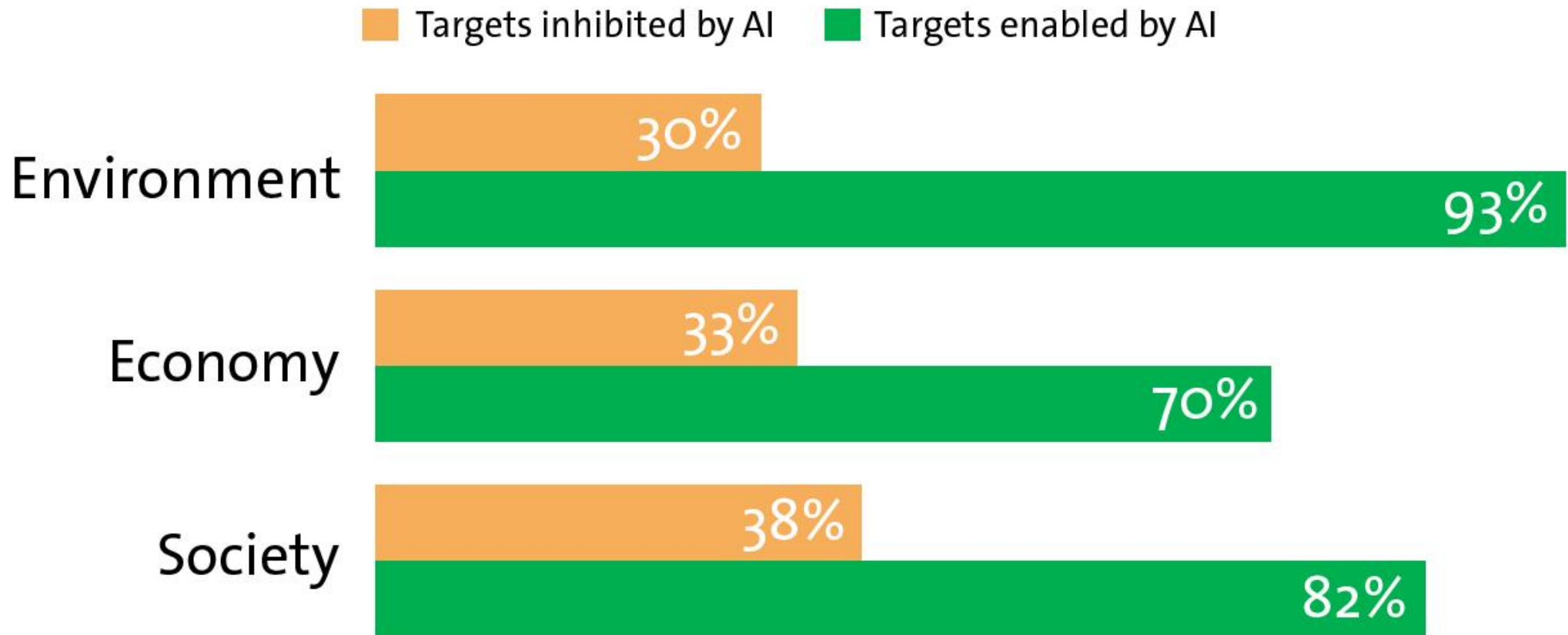


Vinuesa et al., Nature Communications 11, 233 (2020)



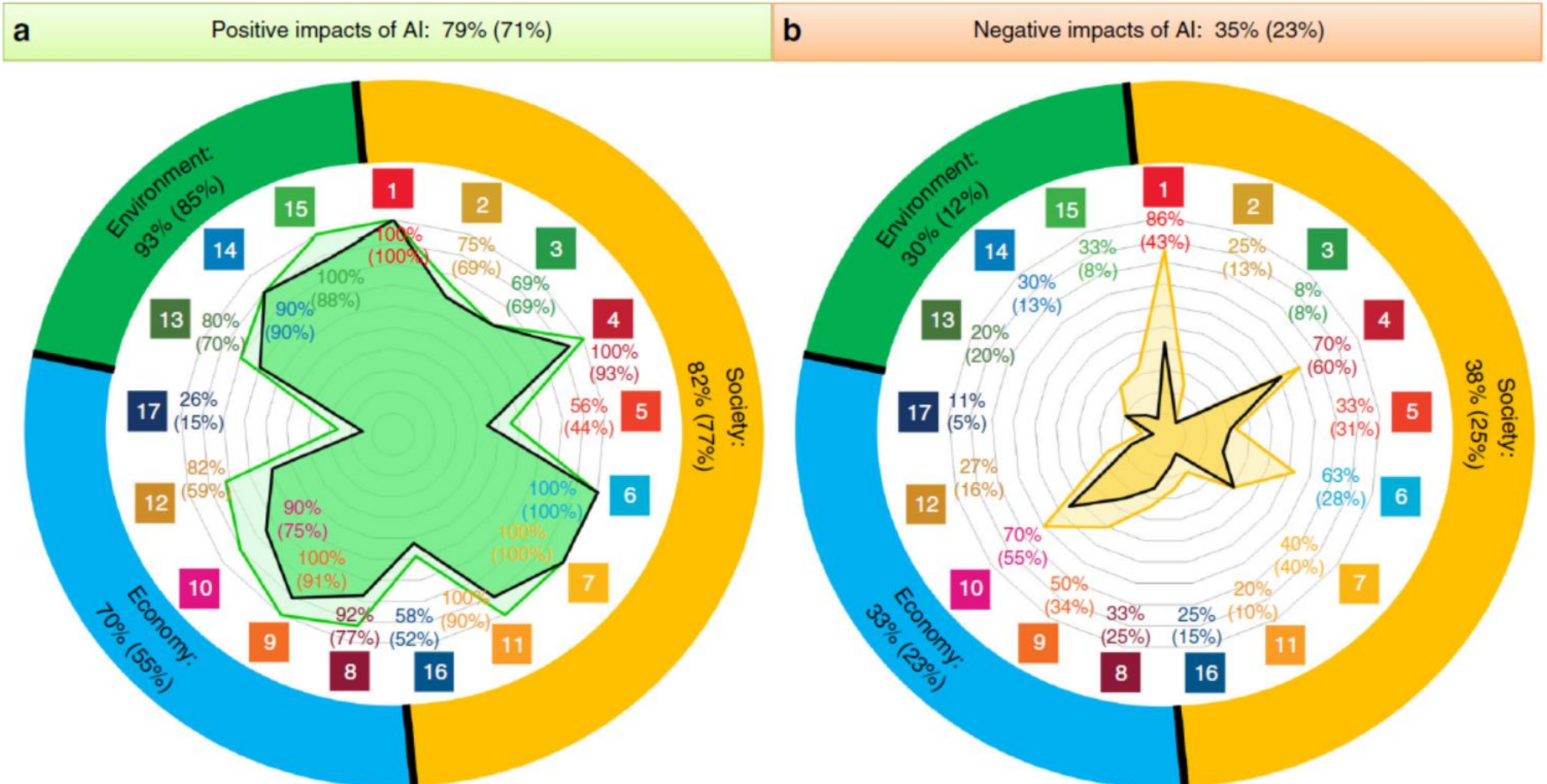
# Impact of AI on each of 169 targets

- We divided the 17 SDGs into 3 main categories (Stockholm Resilience Center, 2017; United Nations (2019): **Society, Economy, and Environment**.
- Percentage of targets where **positive (79%)** or **negative (35%)** impact of AI is documented:



Vinuesa et al., Nature Communications 11, 233 (2020)

– Environment and Society higher reduction of negative; Economy the opposite.



Vinuesa et al., Nature Communications 11, 233 (2020)

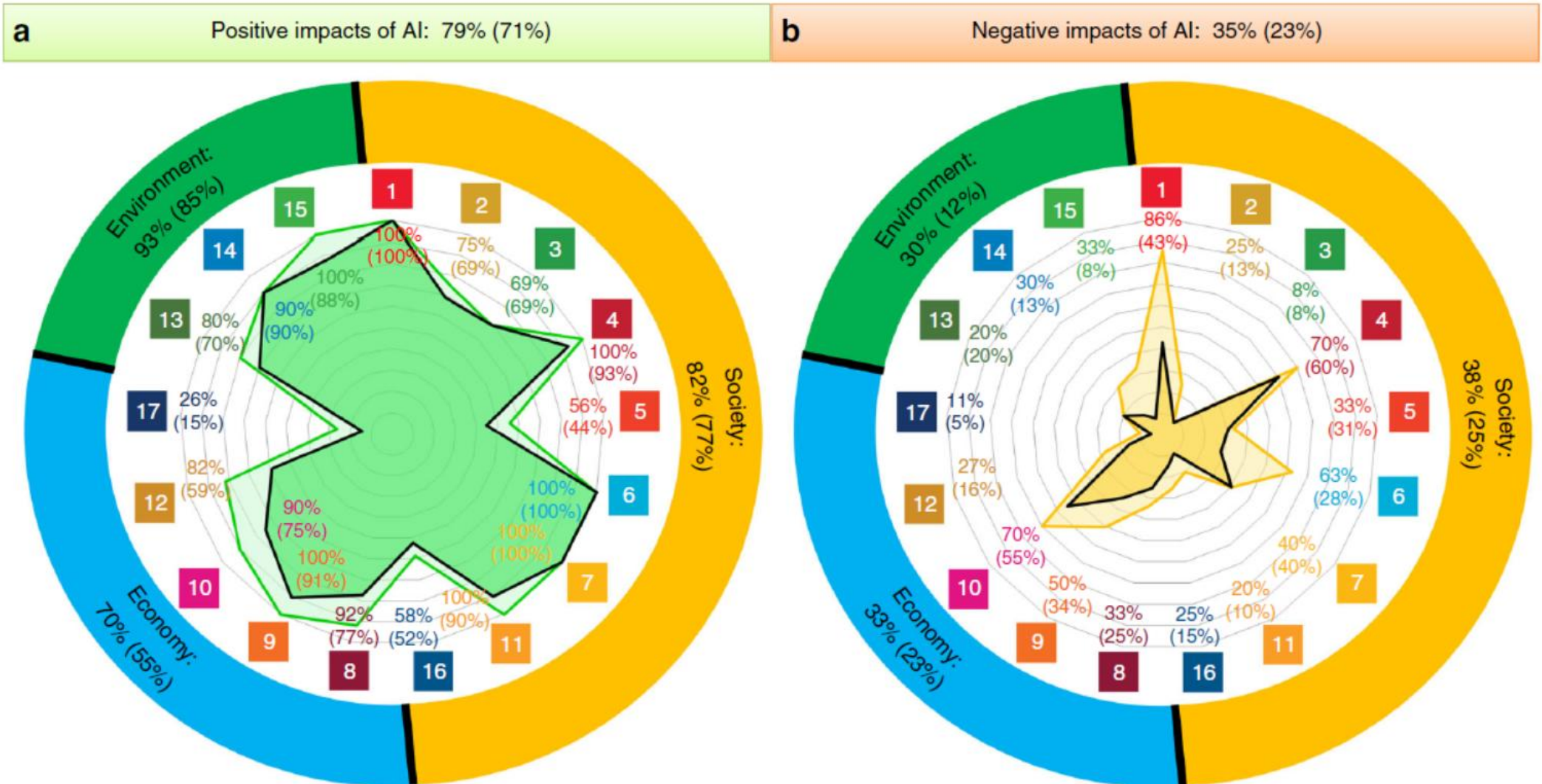


# Types of evidence

- References using sophisticated tools and data to refer to this particular issue and with the possibility to be generalized are of type (A). **1**
- Studies based on data to refer to this particular issue, but with limited generalizability, are of type (B). **0.75**
- Anecdotal qualitative studies and methods are of type (C). **0.5**
- Purely theoretical or speculative references are of type (D). **0.25**

# Types of evidence

– **Environment and Society higher reduction of negative; Economy the opposite.**



Vinuesa et al., Nature Communications 11, 233 (2020)



## Some key results



- **POSITIVE:** AI-enabled technology which may help overcome current barriers (**satellite data** to track poverty, SDG1).



- **NEGATIVE:** Uneven opportunities to access AI resources may end up **increasing inequalities** (SDG 10).

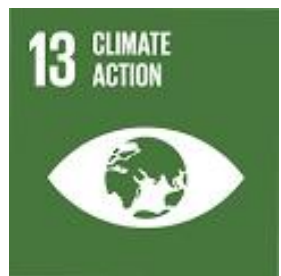


Vinuesa et al., Nature Communications **11**, 233 (2020)



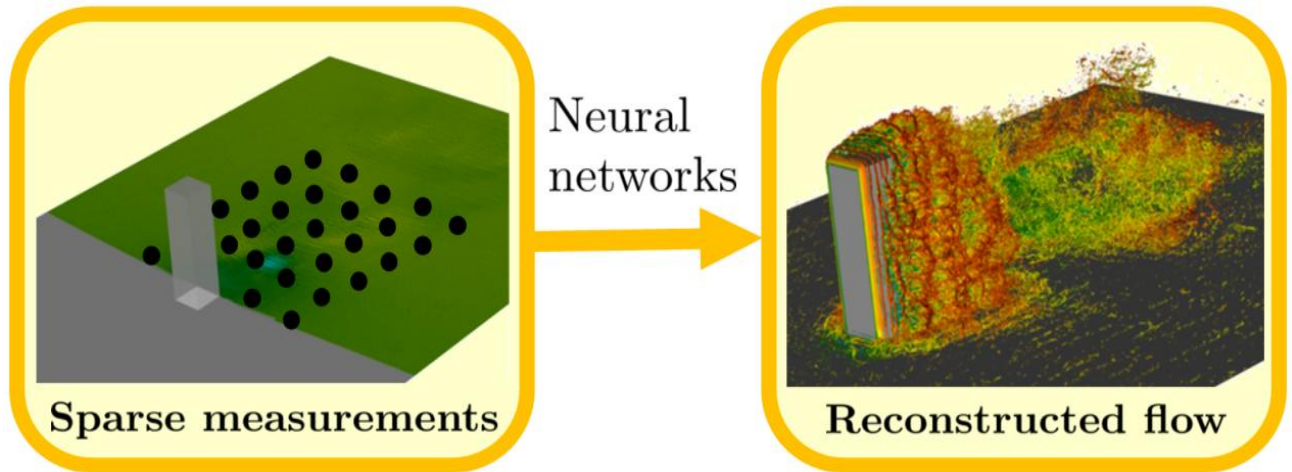
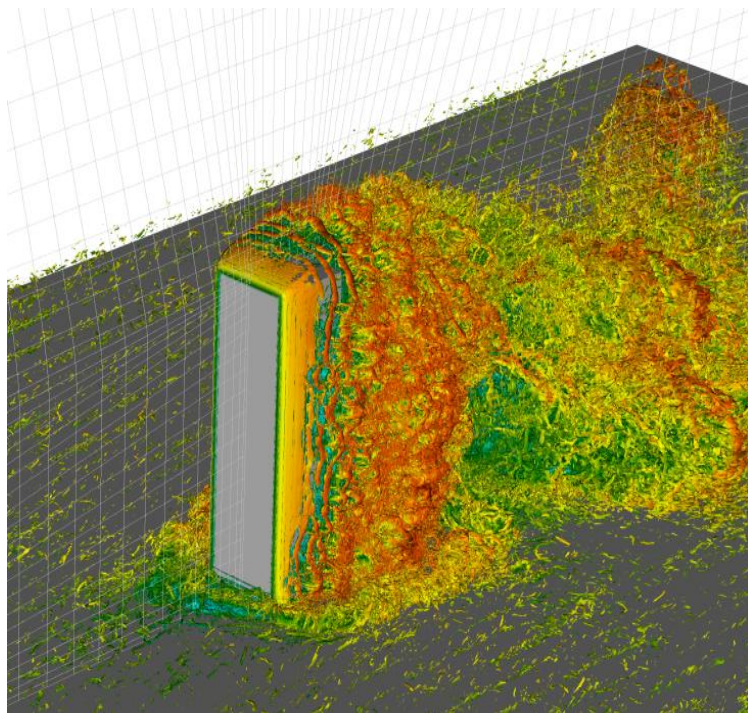
# One application: SDG11 on sustainable cities

- **POSITIVE:** Positive impact of AI on all 10 targets within SDG 11 on sustainable cities. In particular, AI will be able to help us build more accurate and robust **technology to measure air pollution in cities**, which causes 800,000 deaths each year in Europe alone.



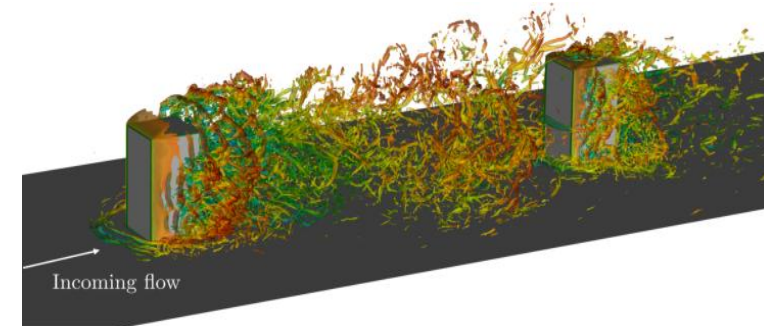
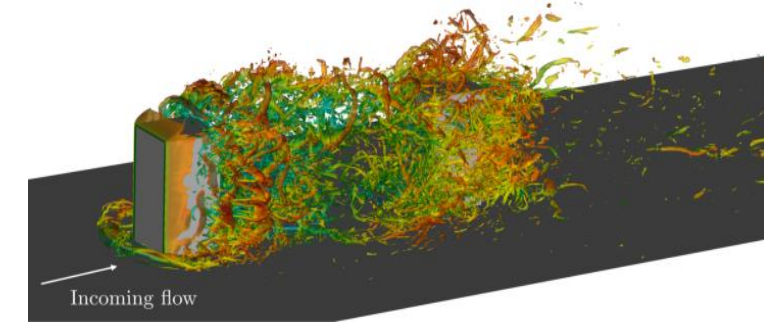
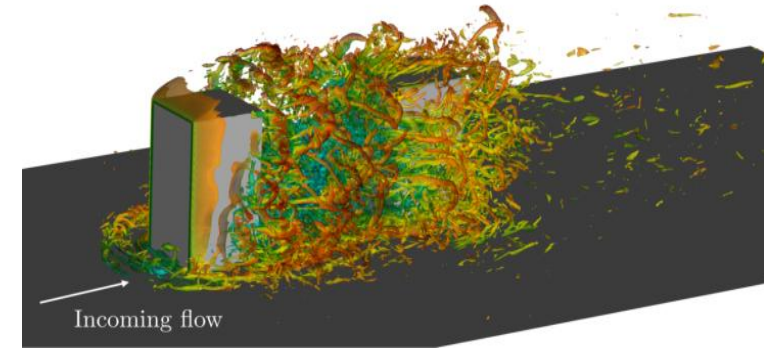
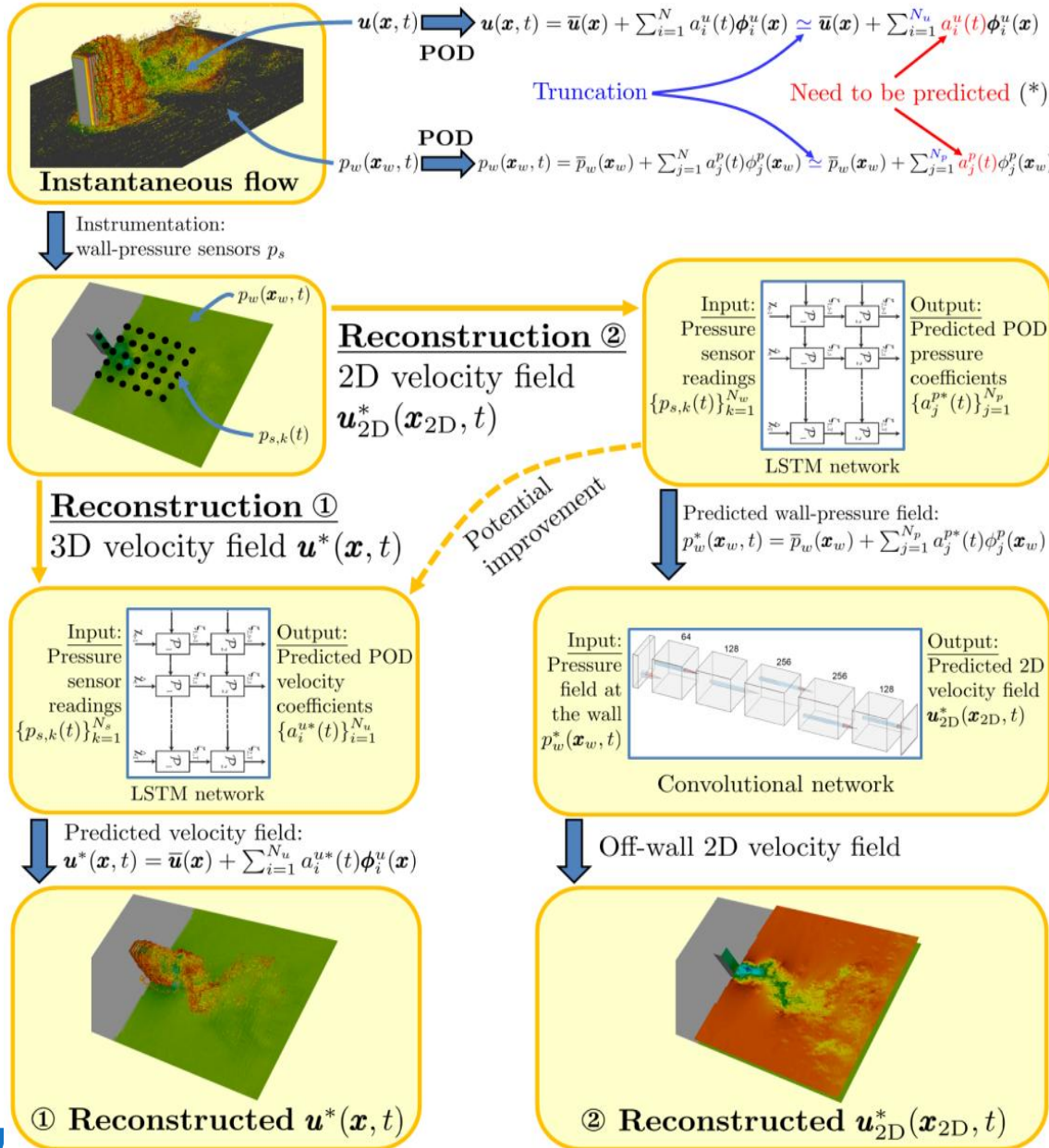
# Non-intrusive sensing in urban flows

- Using highly detailed simulations, we can reproduce the **flow in complex urban environments**.
- Use AI to **improve pollution measurement**.



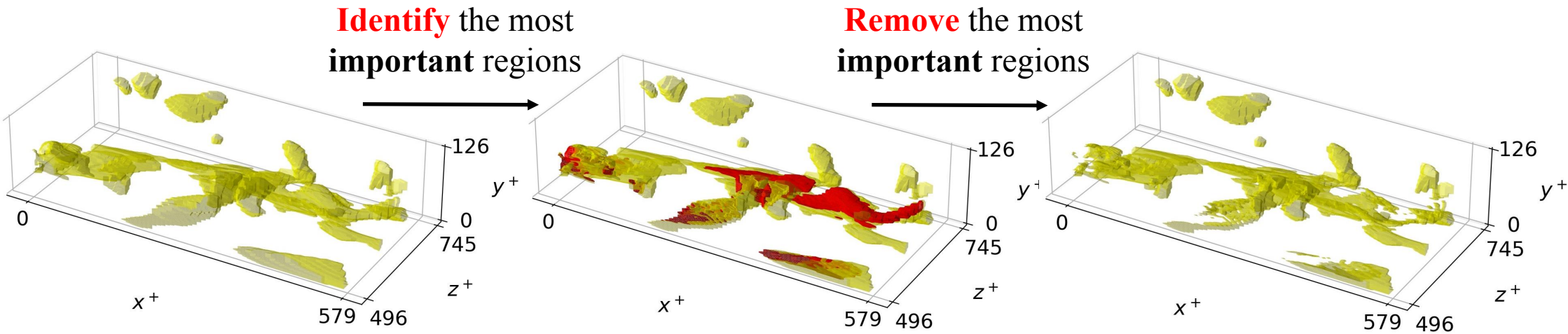
Lazpita et al., Phys. Fluids (2022);  
Martínez-Sánchez et al., IJHFF (2023)

# Non-intrusive sensing in urban flows



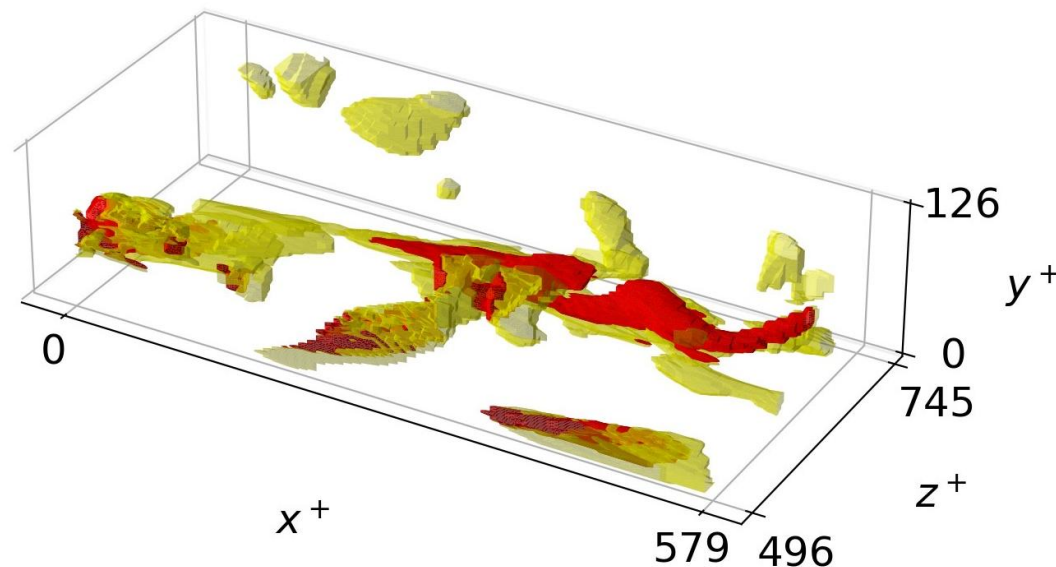
Lazpita et al., Phys. Fluids (2022);  
Martínez-Sánchez et al., IJHFF (2023)

# Reduce pollution, minimize drag... How to control a turbulent flow?



# Outline

- Identify the most important regions with **explainable deep learning (XDL)**.
- Remove the most important regions with deep reinforcement learning (DRL).

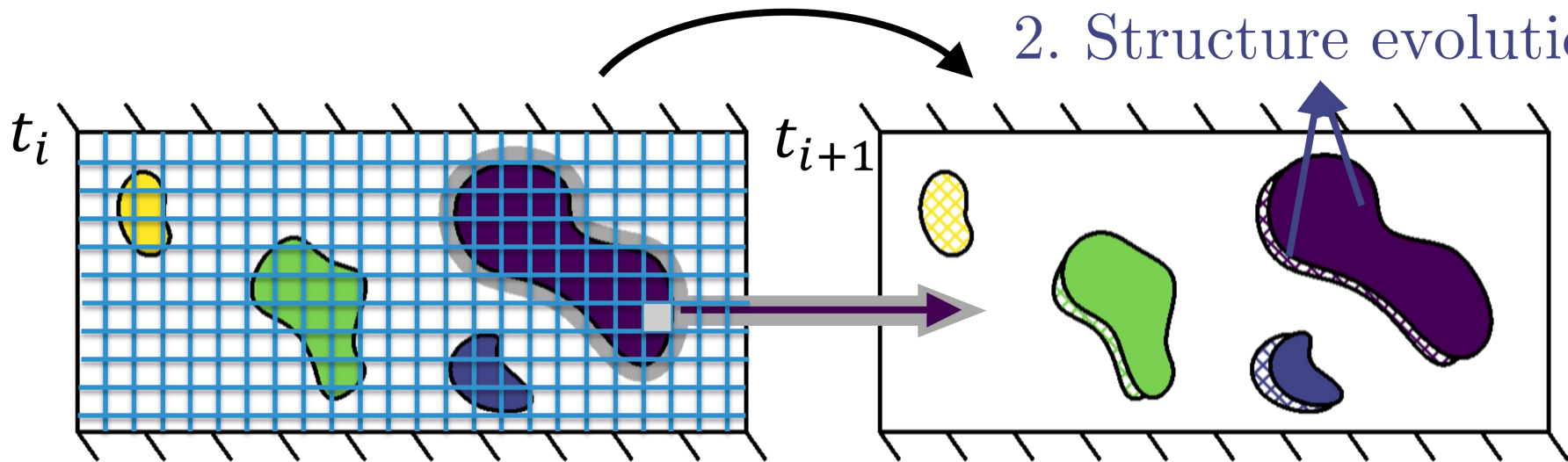


# Which are the most important coherent structures in the flow? XAI framework

1. **Prediction** of a future instantaneous flow field through a **3D U-net**.
2. **Segmentation** of the domain **point by point**.
3. **The importance of each point** for the prediction is assessed by removing it from the field and re-calculating the error. XAI method based on SHapley Additive exPlanations (**SHAP**). ⇒ **By Lundberg and Lee (2017), very well established in ML (>30k citations).**

1. DNN flow prediction

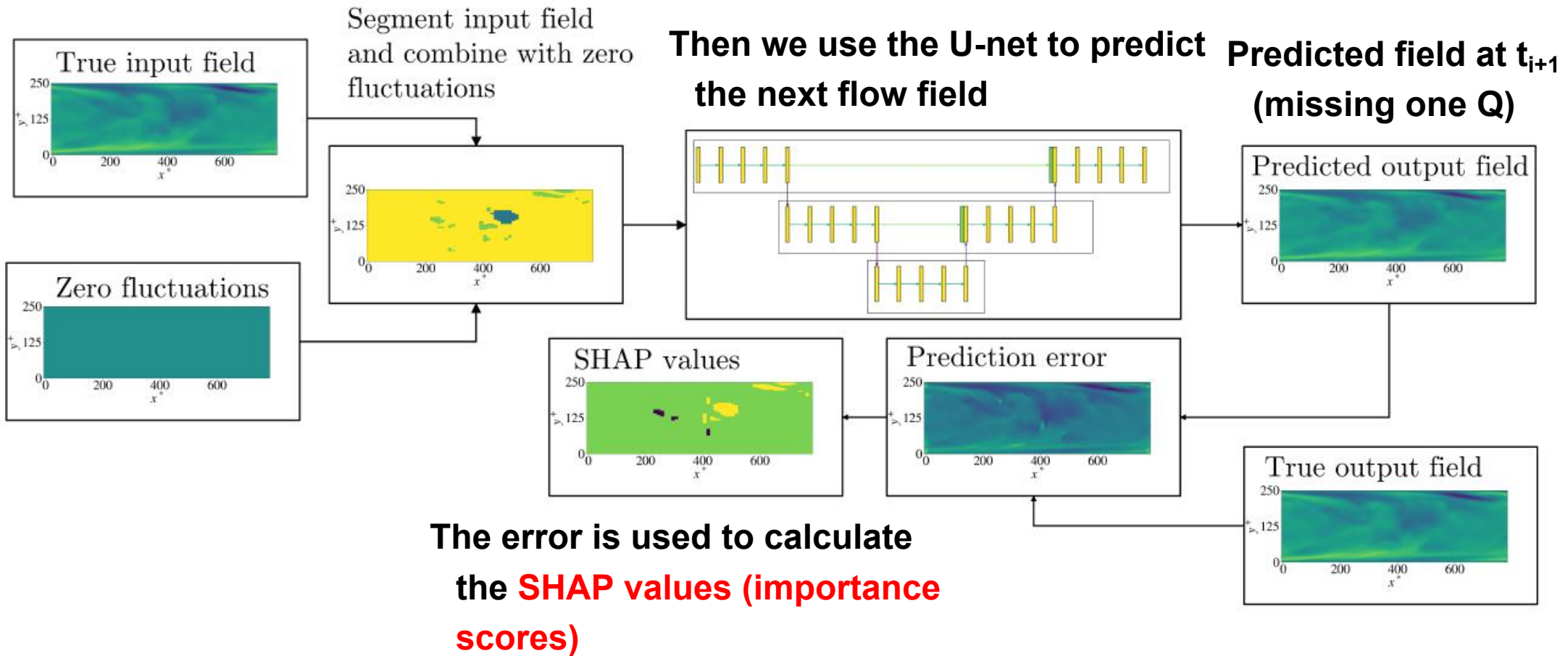
2. Structure evolution



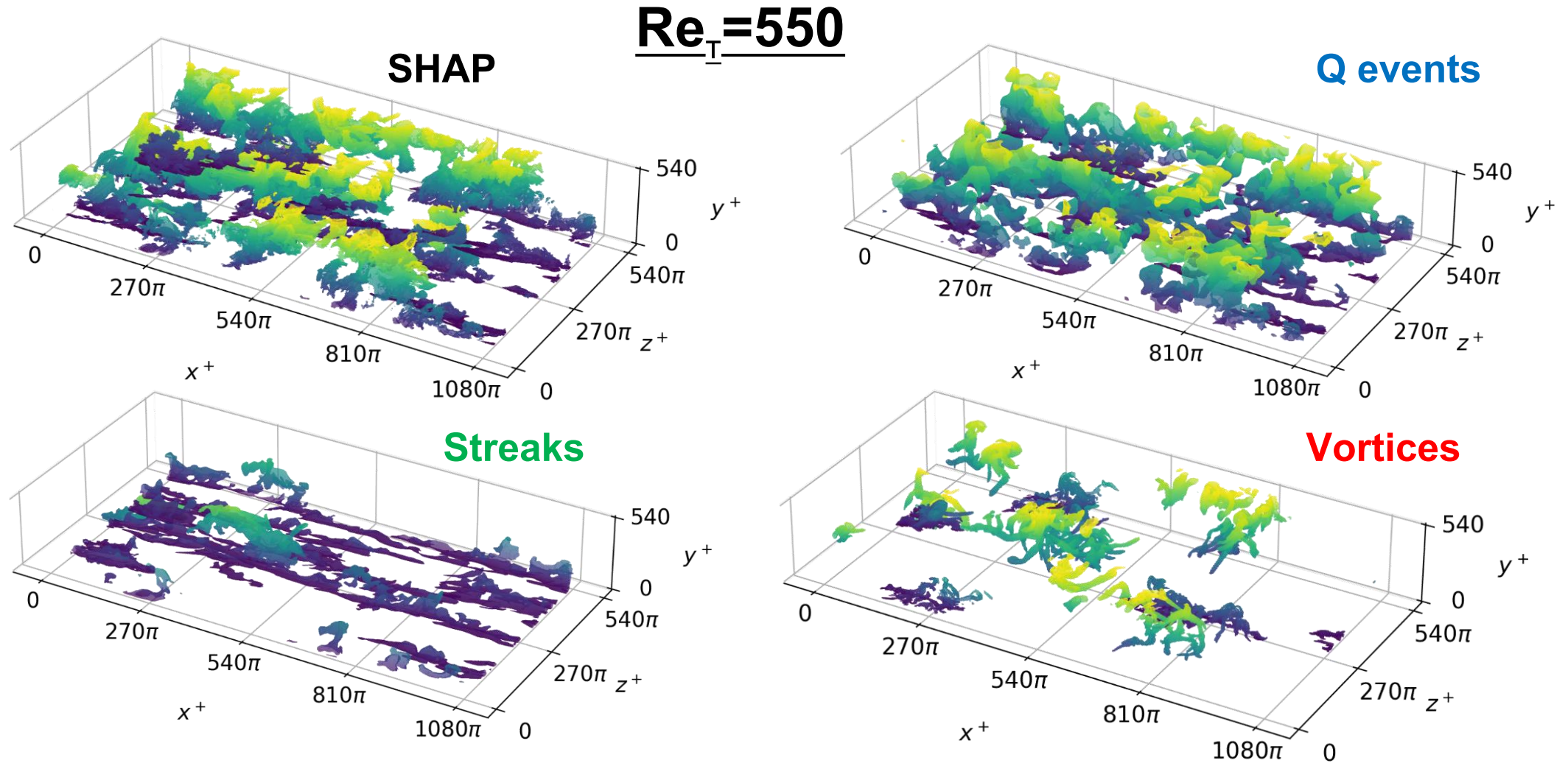
3. Pixel contribution to the prediction (SHAP)

# Explainability algorithm

For each Q structure, we substitute its volume by zero fluctuations



# Applying SHAP point by point to 3D DNS data. Comparison with other structures

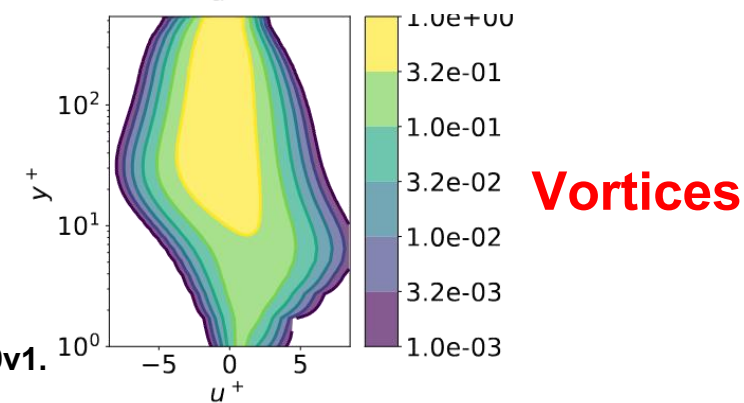
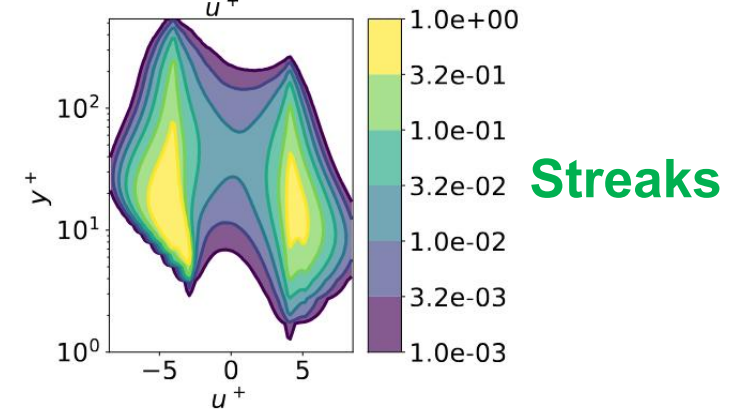
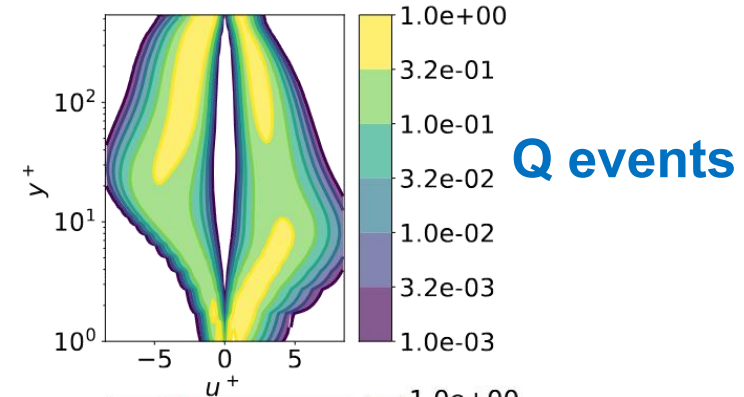
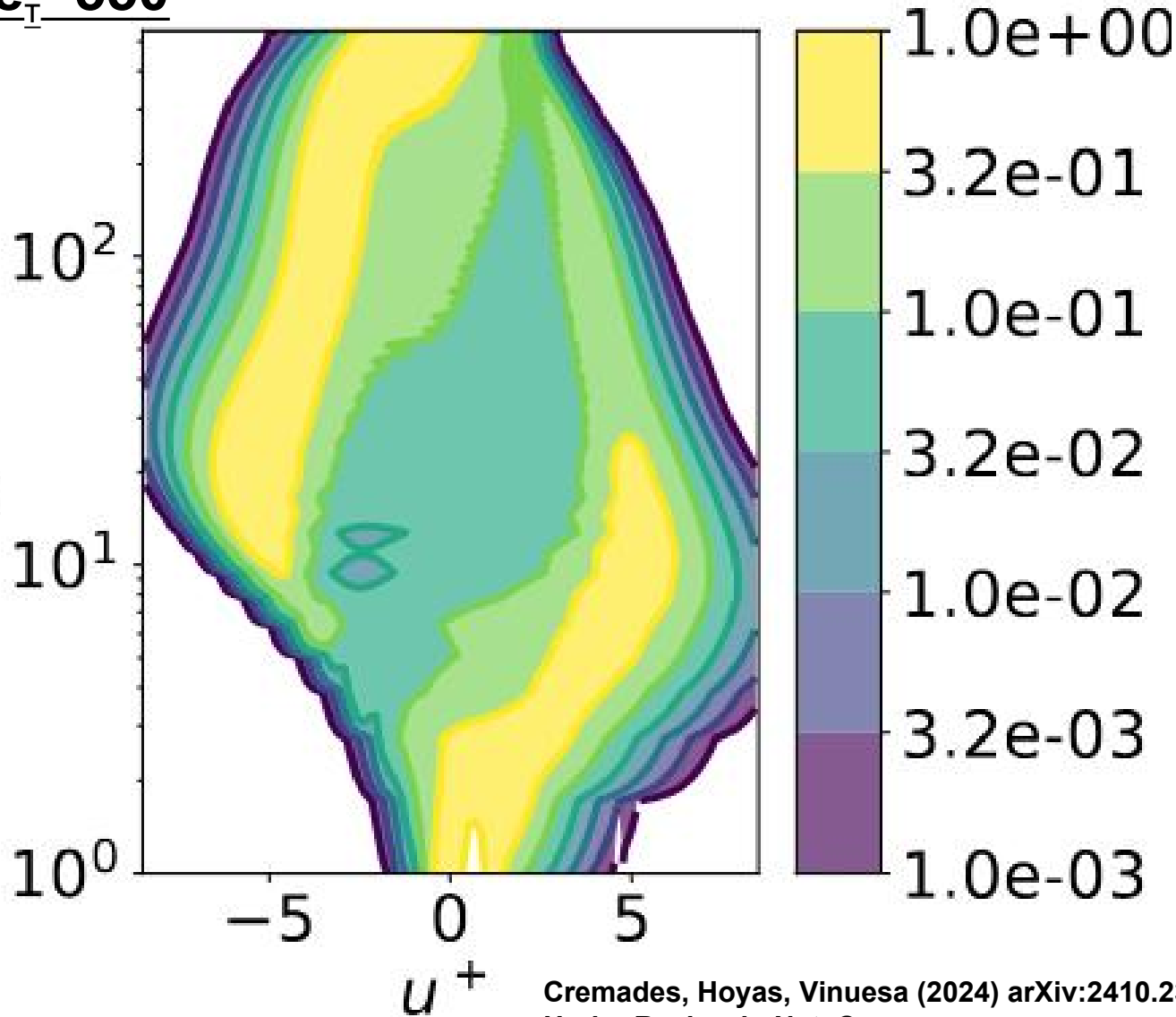


Cremades, Hoyas, Vinuesa (2024), Preprint arXiv:2410.23189v1  
(Under Review in Nat. Commun.)

# SHAP point by point in the 3D DNS data: $u'$ . Similarities with other structures

$Re_T = 550$

SHAP



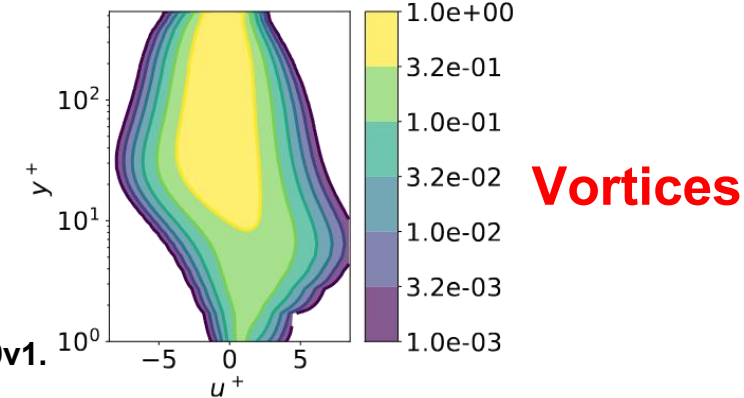
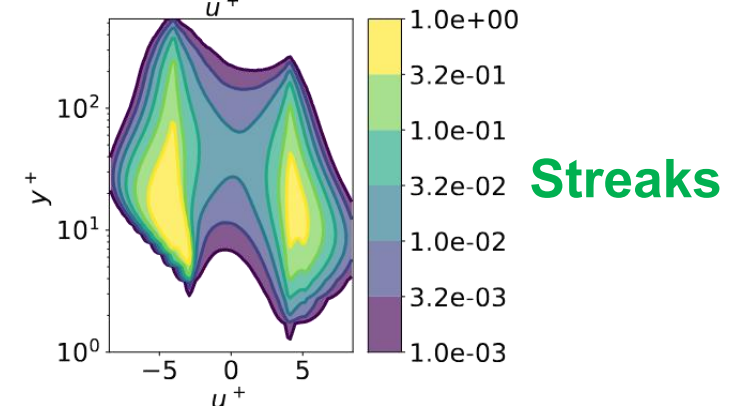
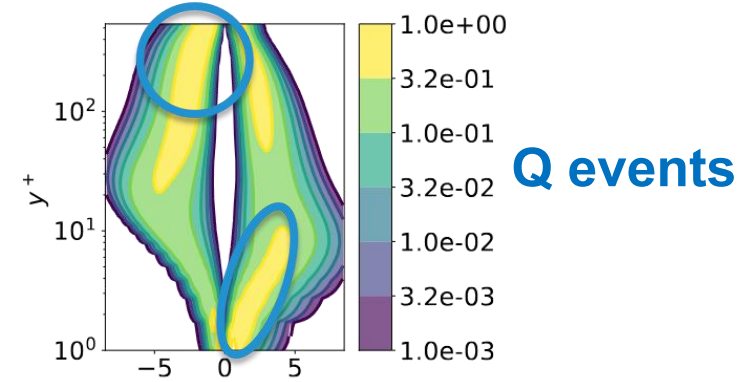
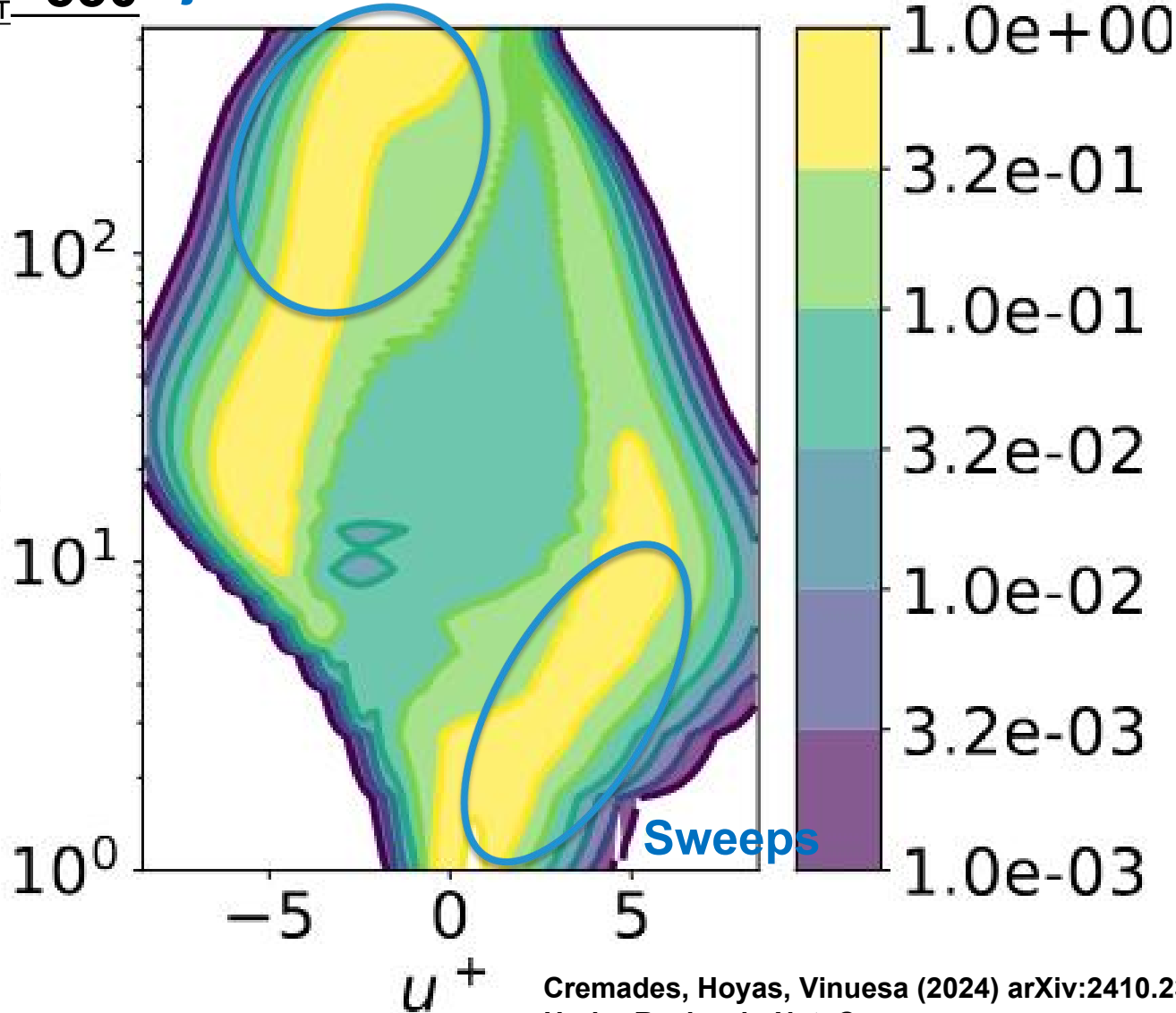
Cremades, Hoyas, Vinuesa (2024) arXiv:2410.23189v1.  
Under Review in Nat. Commun.

# SHAP point by point in the 3D DNS data: $u'$ . Similarities with other structures

$Re_T = 550$

Ejections

SHAP

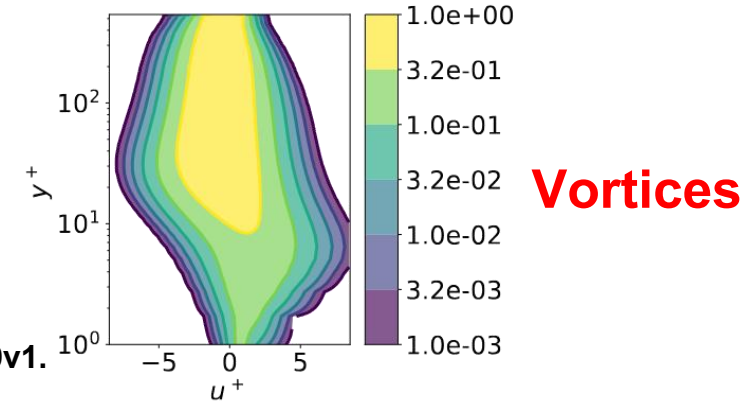
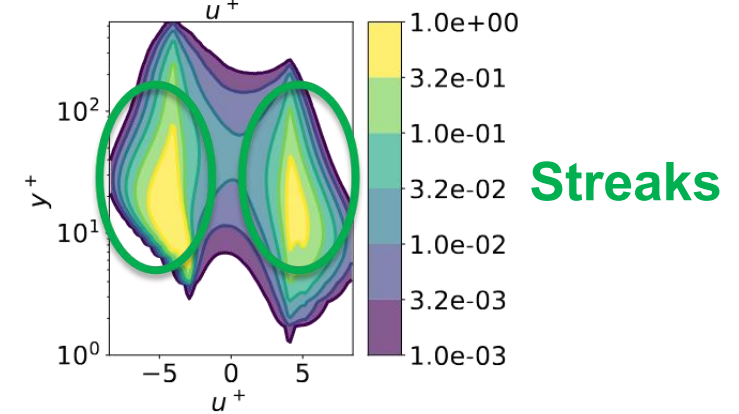
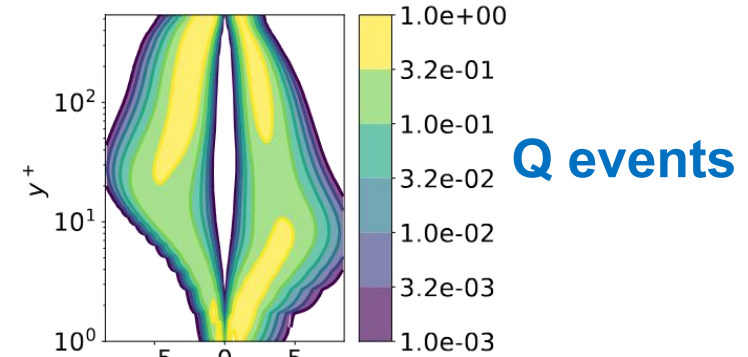
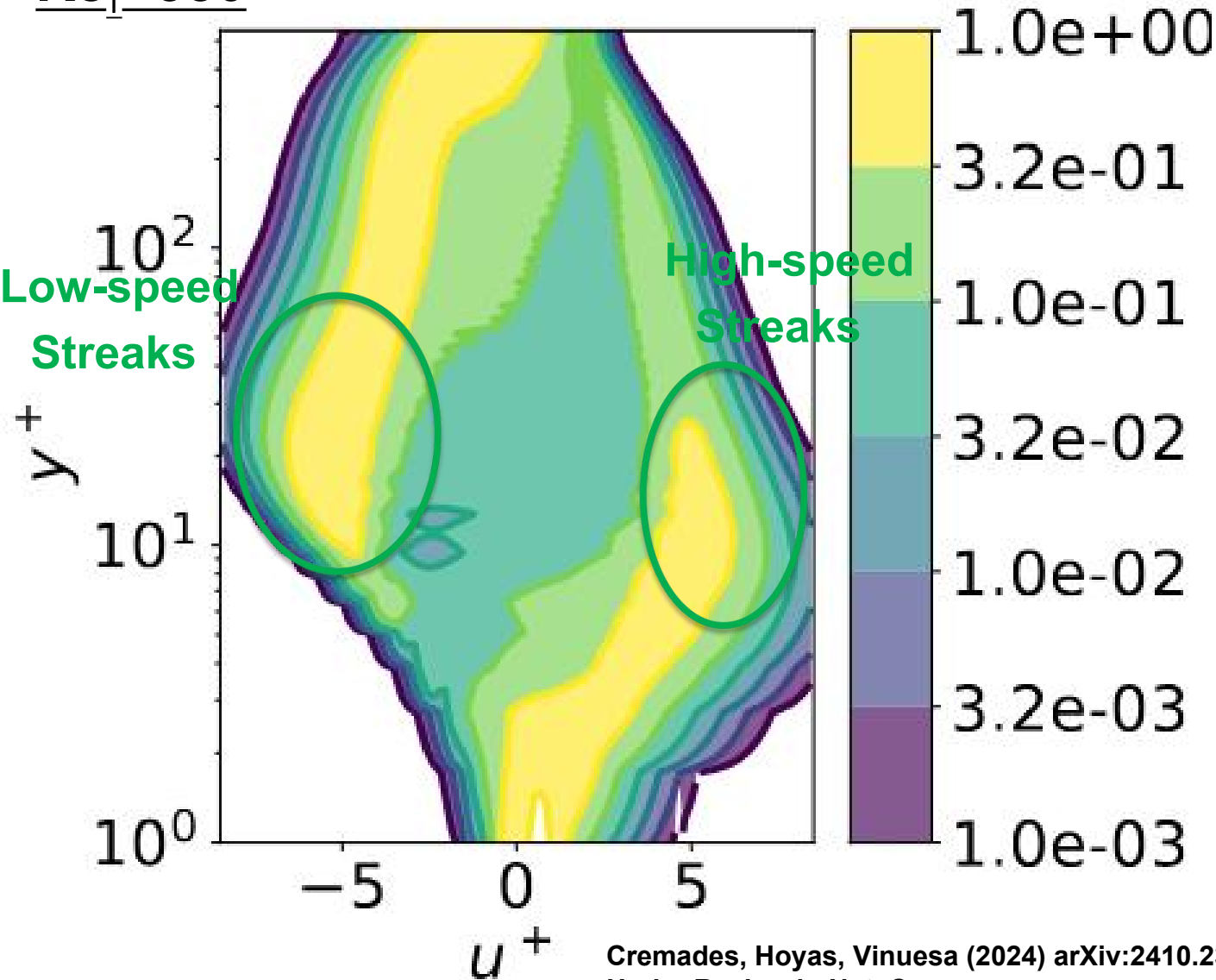


Cremades, Hoyas, Vinuesa (2024) arXiv:2410.23189v1.  
Under Review in Nat. Commun.

# SHAP point by point in the 3D DNS data: $u'$ . Similarities with other structures

$Re_T = 550$

SHAP

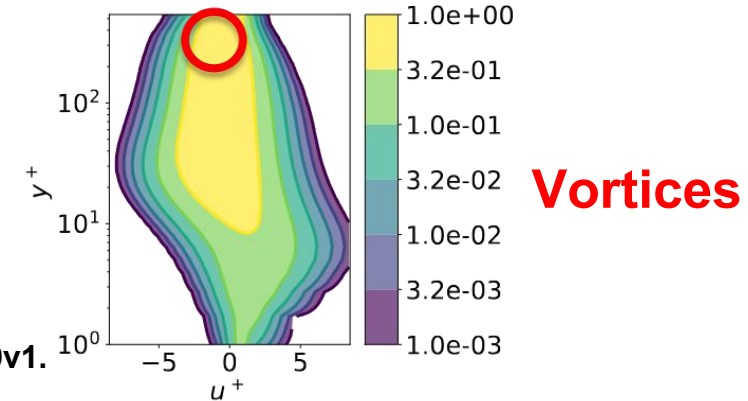
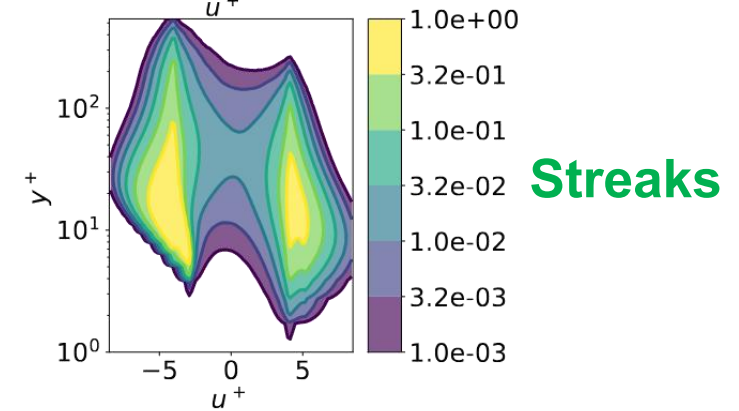
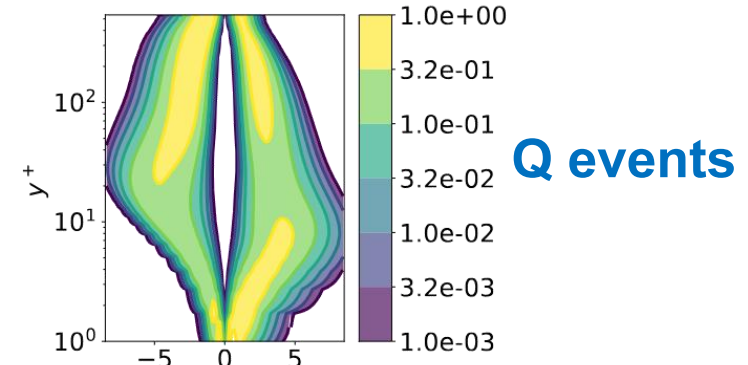
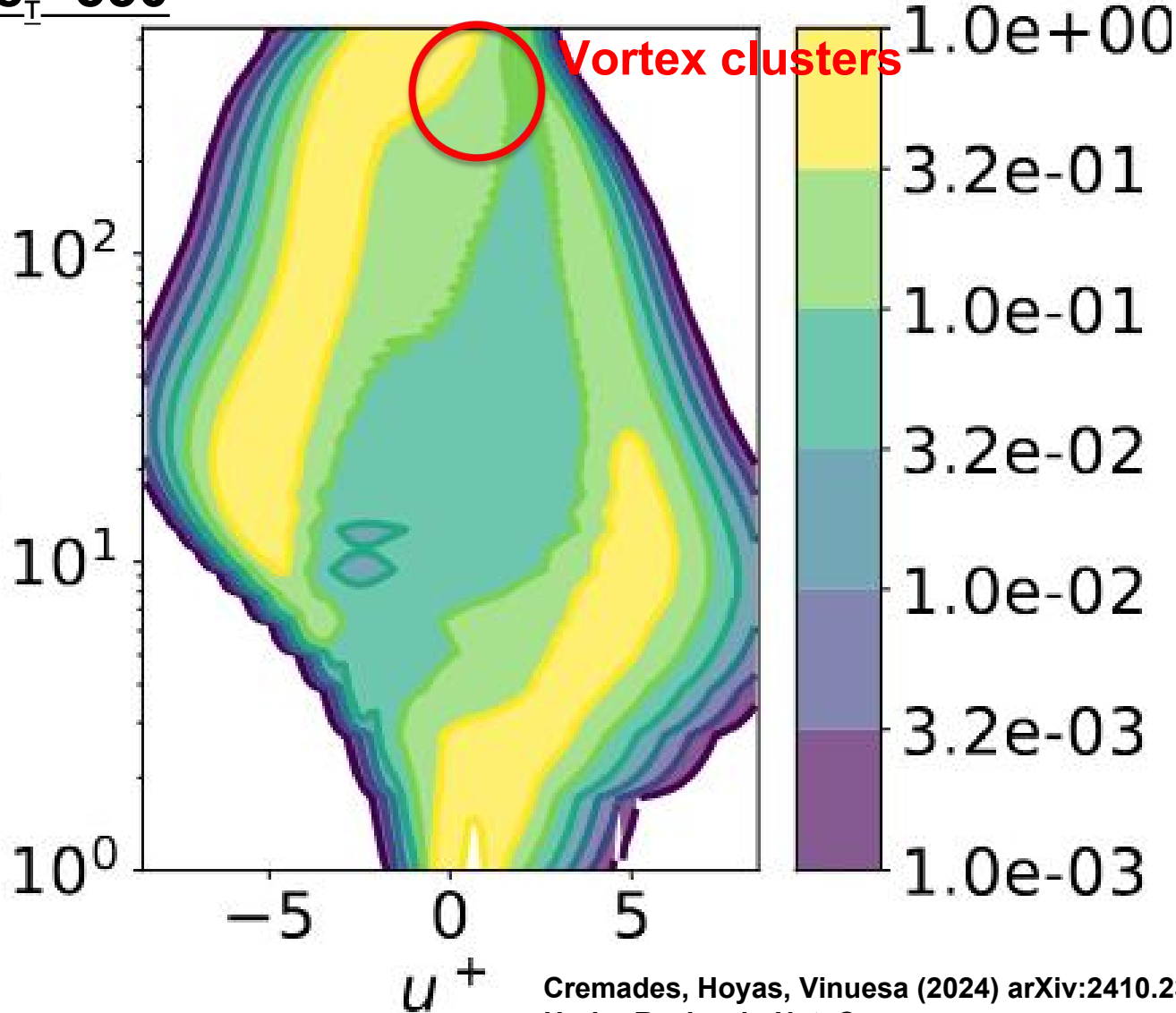


Cremades, Hoyas, Vinuesa (2024) arXiv:2410.23189v1.  
Under Review in Nat. Commun.

# SHAP point by point in the 3D DNS data: $u'$ . Similarities with other structures

$Re_T = 550$

SHAP



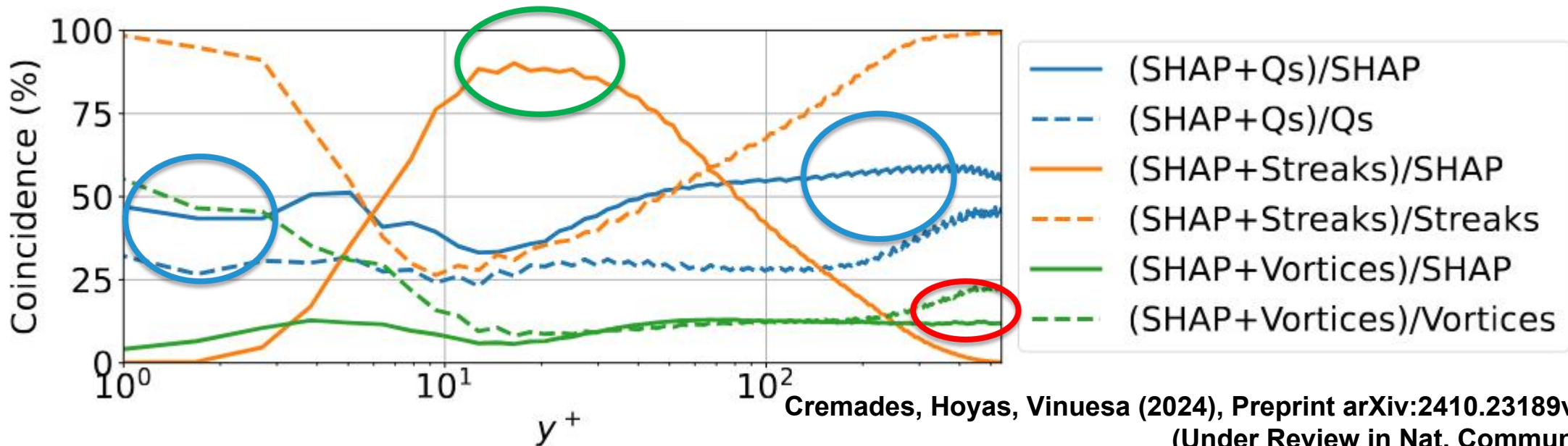
Cremades, Hoyas, Vinuesa (2024) arXiv:2410.23189v1.  
Under Review in Nat. Commun.



# One-to-one comparison between SHAP and other structures

$Re_T=550$

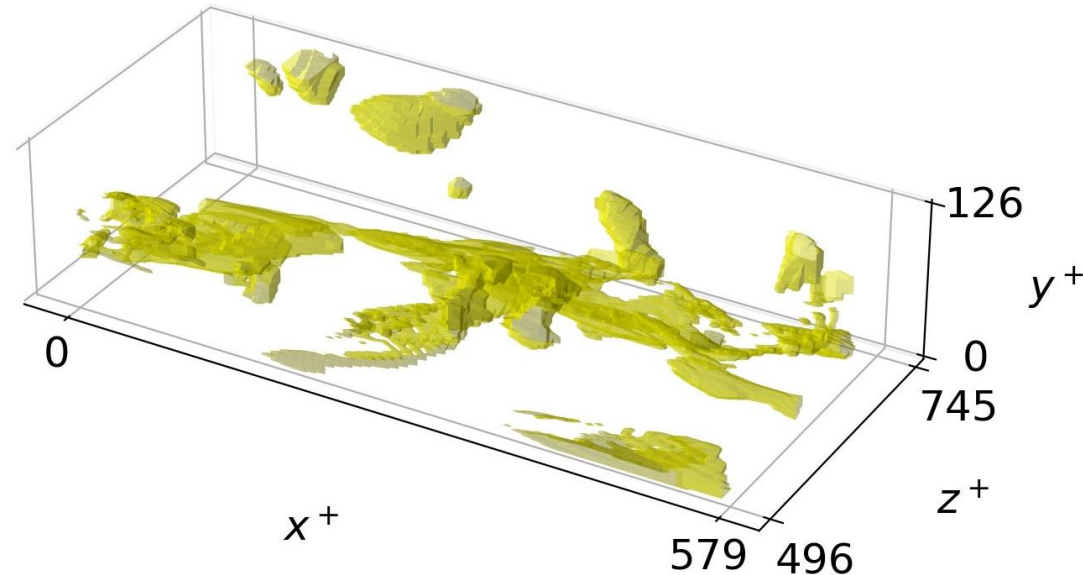
- At  $y^+=15$ , the **SHAP structures are basically streaks (around 90% coincidence)**.
- Close to the **wall and channel center**, the **agreement between SHAP and Q events is around 50% (ejections and sweeps)**.
- At the **channel center**, the SHAP structures exhibit a **modest agreement (around 15%) with the vortices**.
- **The classically studied coherent structures only paint a partial picture of wall-bounded turbulence!**



Cremades, Hoyas, Vinuesa (2024), Preprint arXiv:2410.23189v1  
(Under Review in Nat. Commun.)

# Outline

- Identify the most important regions with explainable deep learning (XDL).
- Remove the most important regions with **deep reinforcement learning (DRL)**.

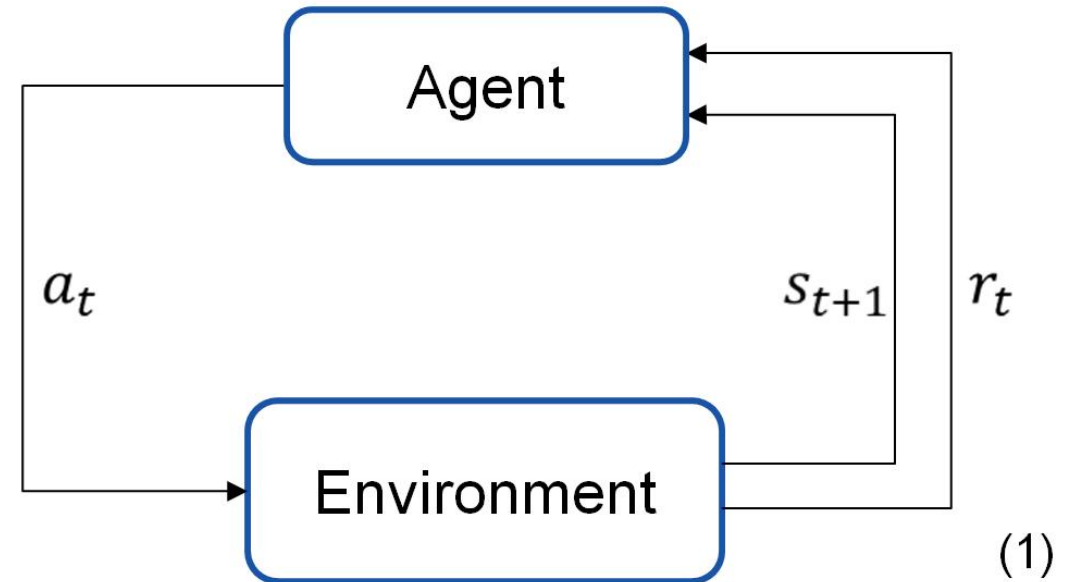


# Reinforcement learning for flow control

## Introduction

- Constituting elements:
  - Agent
  - Environment
  - State space  $S = \{s_1, s_2, \dots, s_N\}$
  - Action space  $A = \{a_1, a_2, \dots, a_M\}$
  - Transition function  $\mathbb{P}(s_{t+1}|s_t, a_t)$
  - Reward function  $r_t = R(s_t, a_t, s_{t+1})$
- Goal:

*“Define a policy  $\pi(a_t|s_t)$  that maximizes the reward”*



1. Sutton, R.S. Learning to predict by the methods of temporal differences. *Mach Learn* 3, 9–44 (1988)

**Guastoni et al., Eur. Phys. J. E, 46, 27 (2023)**

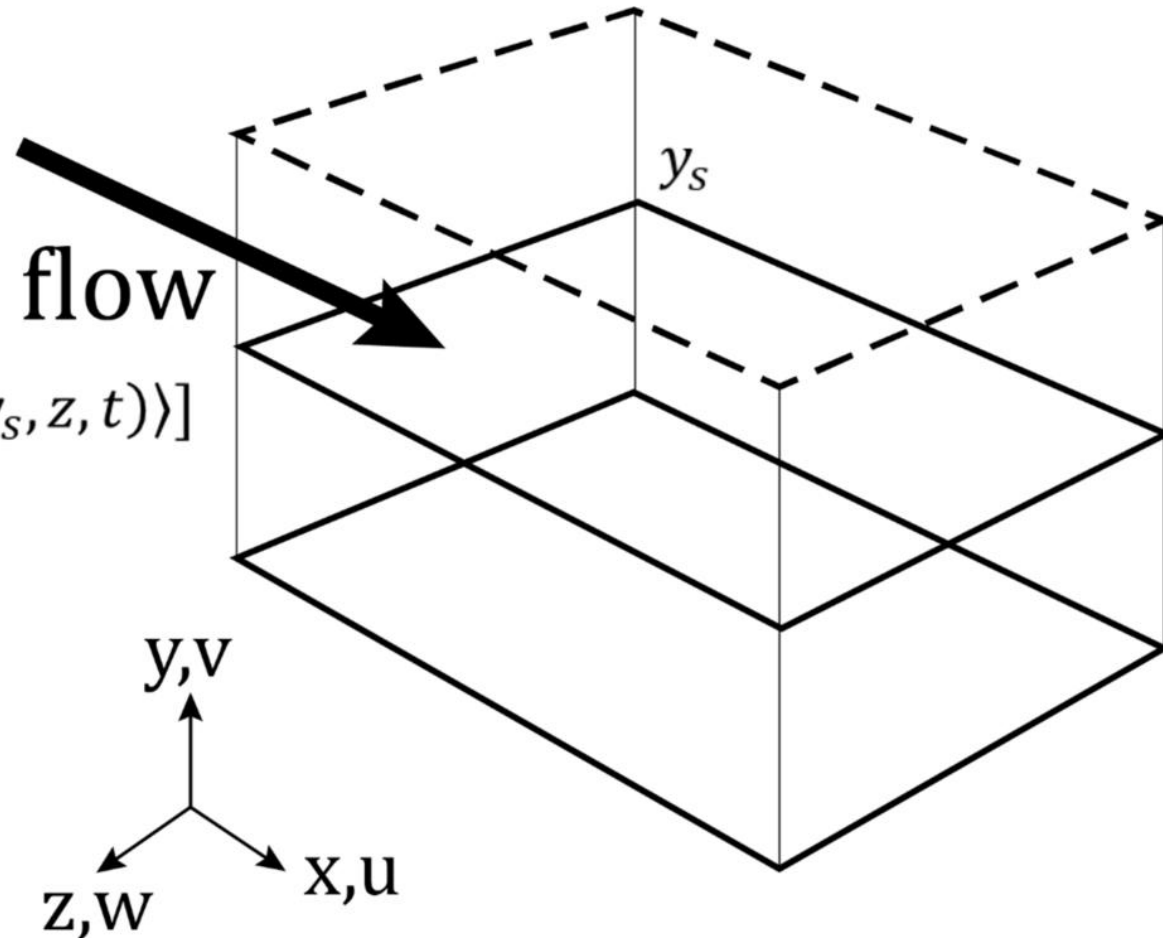
**Vignon et al., Phys. Fluids, 35, 031301 (2023)**

# Baseline: opposition control

- Introduced by Choi *et al.*<sup>1</sup>
- Reactive control to reduce the wall-normal fluctuations

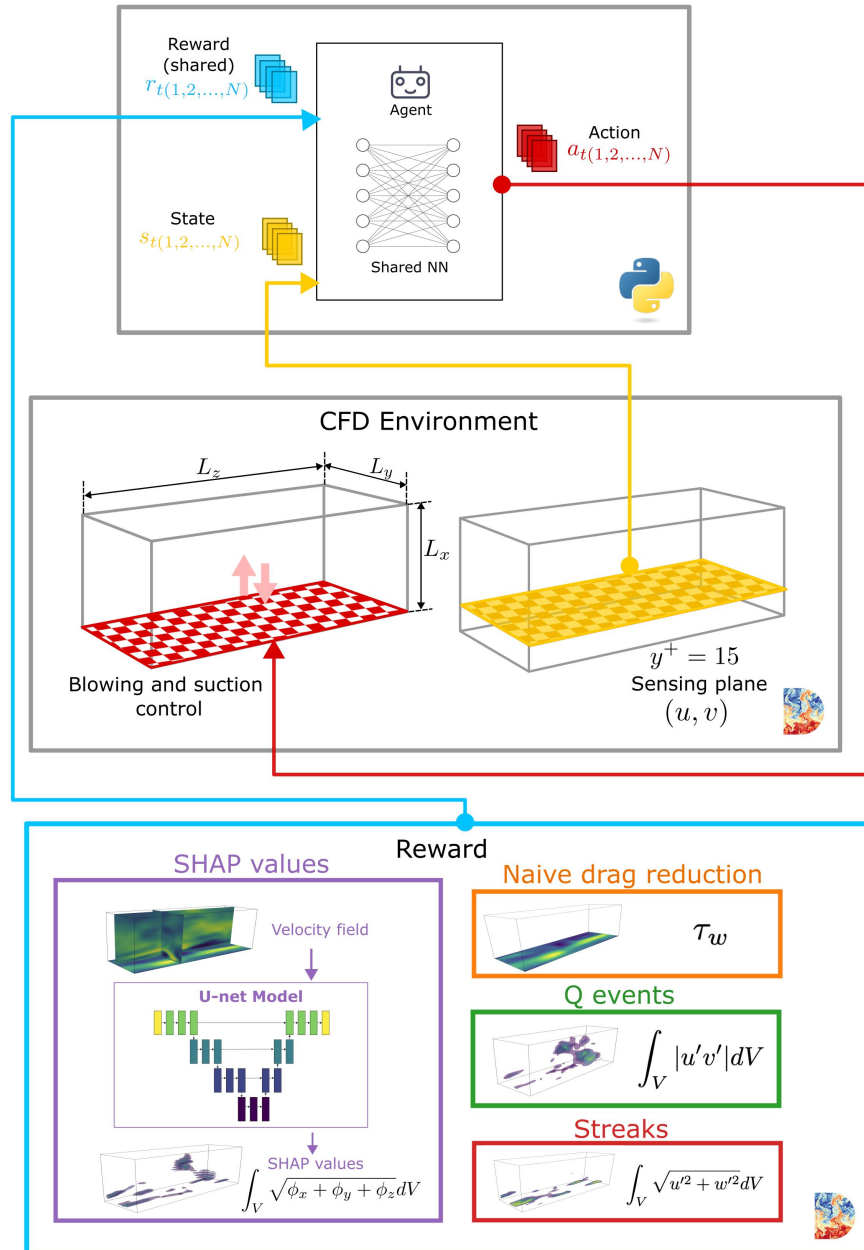
$$v_{wall}(x, z, t) = -\alpha[v(x, y_s, z, t) - \langle v(x, y_s, z, t) \rangle]$$

- $y_s$  wall-normal location of the sensing-plane
- $\alpha$  positive scaling parameter



1. Choi, H., Moin, P., & Kim, J. (1994). Active turbulence control for drag reduction in wall-bounded flows. *Journal of Fluid Mechanics*, 262, 75-110

# DRL control targeting SHAP structures



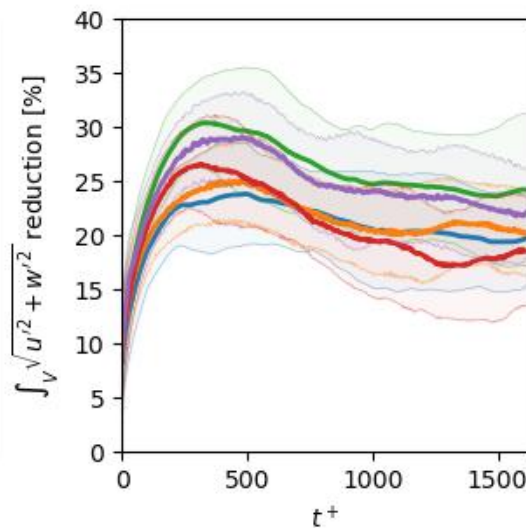
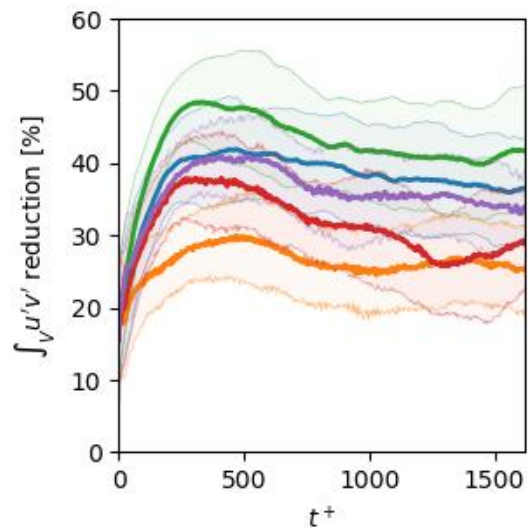
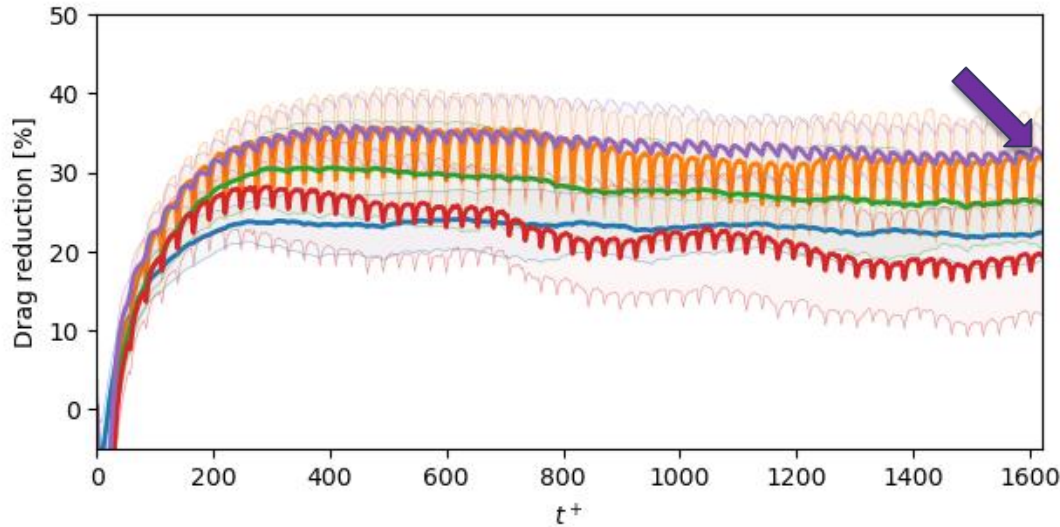
## Comparison of control cases

- Opposition control (baseline)
- DRL reward: wall-shear-stress reduction
- DRL reward: Q-event reduction
- DRL reward: streak reduction
- DRL reward: SHAP reduction

Beneitez et al.,  
Preprint arXiv:2504.02354 (2025)

# DRL control targeting SHAP structures

## Drag reduction



### Comparison of control cases

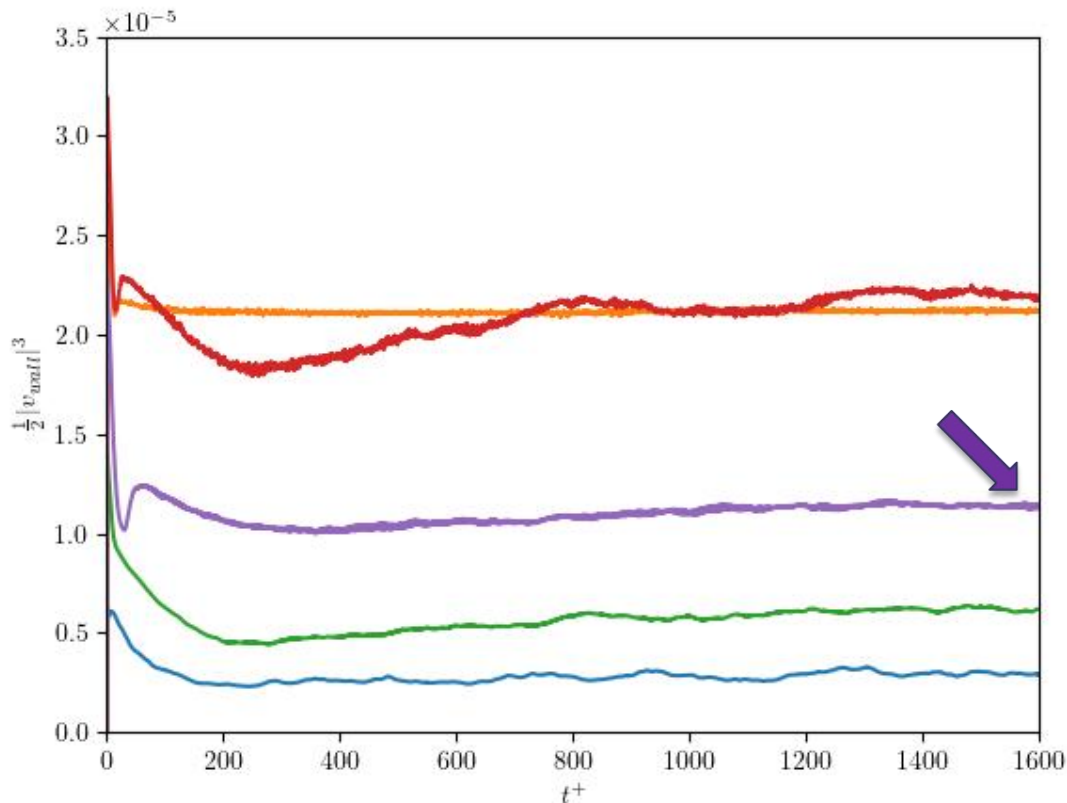
- Opposition control (baseline): 23%
- DRL reward, wall-shear-stress reduction: 31.7%
- DRL reward, Q-event reduction: 27.5%
- DRL reward, streak reduction: 21.2%
- DRL reward, SHAP reduction: 33.3% (more stable than just DRL, 1.6 pp and 5% better).



# DRL control targeting SHAP structures

## Net energy saving

$$S = \frac{c_{f,\text{uncontrolled}} - (c_f + w_{\text{in}})}{c_{f,\text{uncontrolled}}}$$



### Comparison of control cases

- Opposition control (baseline): 22.96%
- DRL reward, wall-shear-stress reduction: 31.4%
- DRL reward, Q-event reduction: 27.47%
- DRL reward, streak reduction: 21%
- DRL reward, SHAP reduction: 33.1% (half the power than just DRL, 1.7 pp and 5.4% better).



Beneitez et al., Preprint arXiv:2504.02354 (2025)



# Summary and Conclusions

- AI can help to achieve 79% of the SDG targets, but can be an inhibitor to 35%. **Very much needed global debate.**
- The **SHAP method** is intrusive for the surrogate, and can be applicable to data-scarce environments (e.g. experiments). **Identification of new coherent structures based on SHAP.**
- Using the **SHAP-based structures as the reward** yields the highest drag reduction through DRL!!

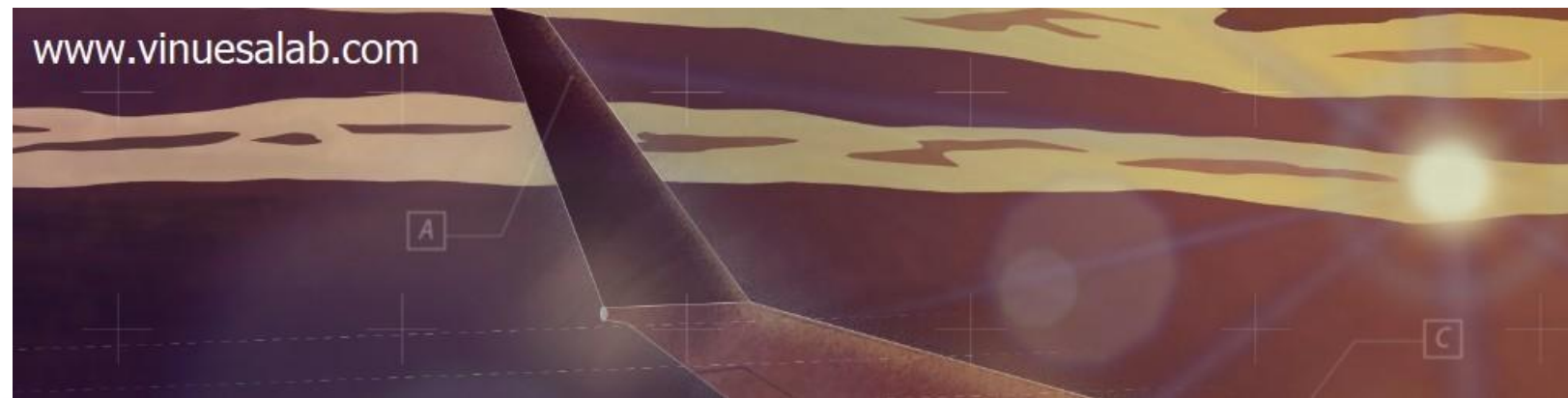
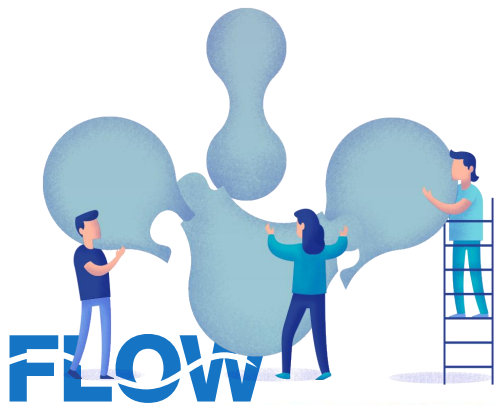
GitHub



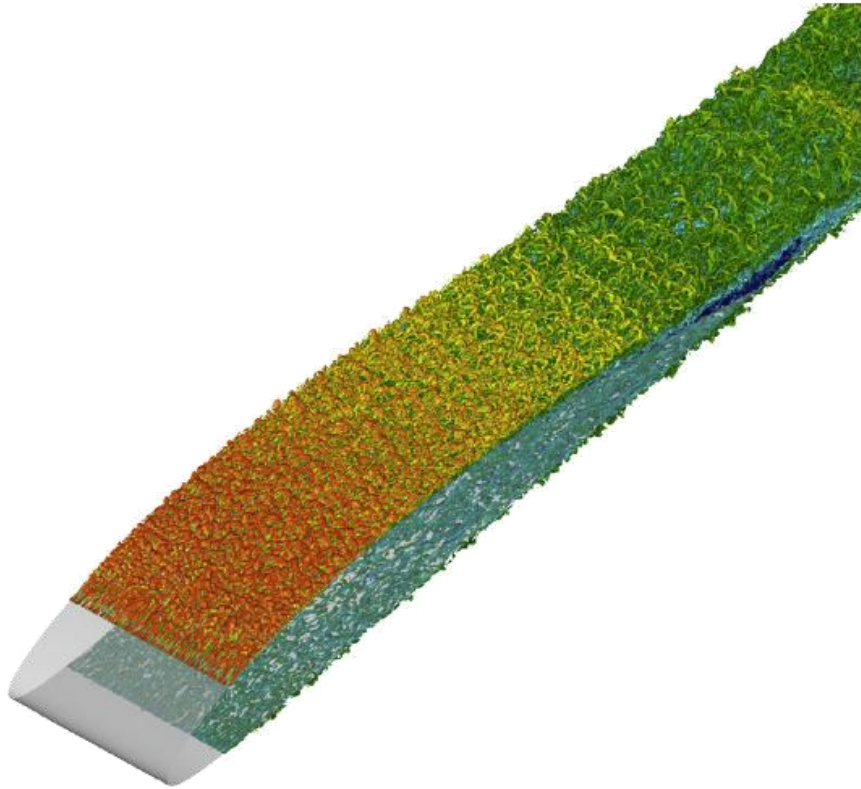
Ricardo Vinuesa



@ricardovinuesa



# DRL control of skin friction in turbulent wings NACA4412 wing at $Re_c=200,000$ , $AoA=5$ deg.



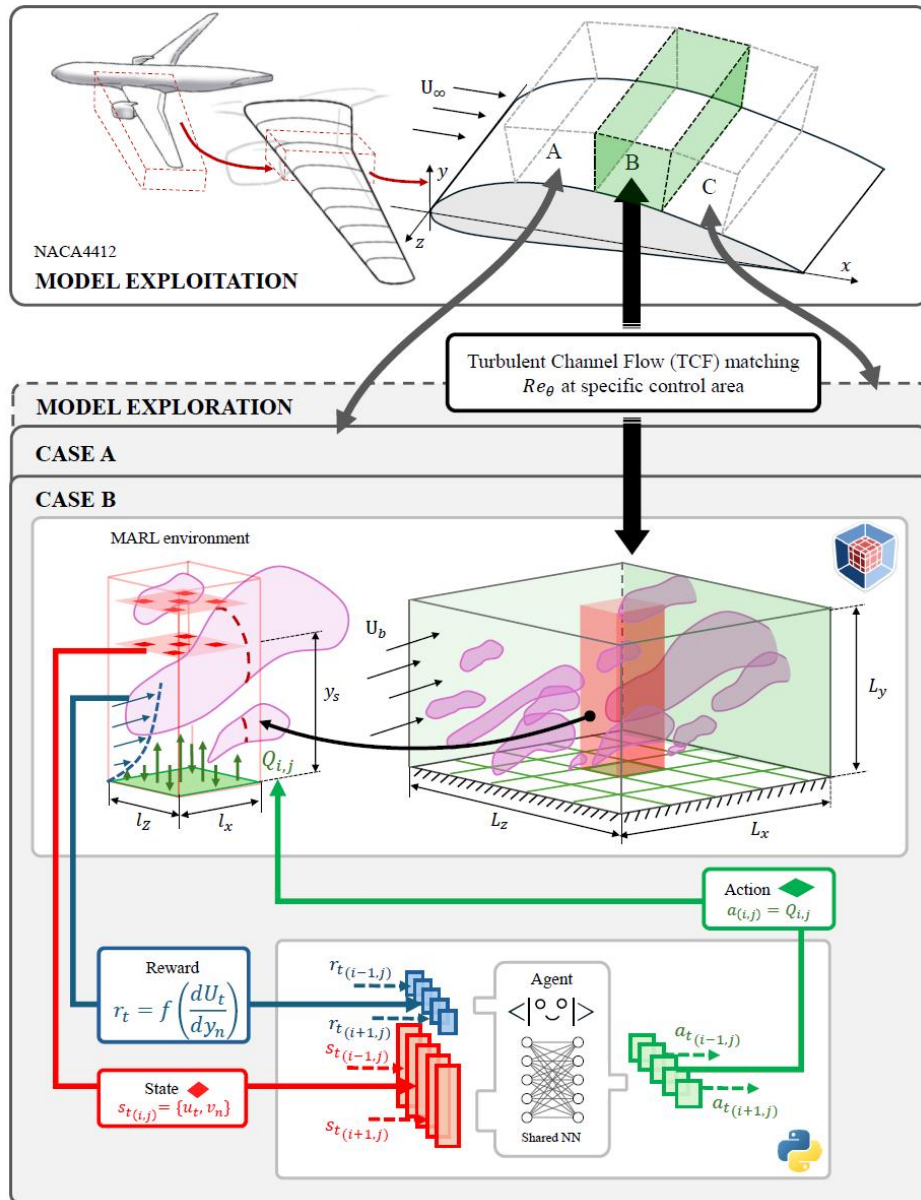
Vinuesa et al., IJHFF 72, 86 (2018)

## Problems applying MARL to a turbulent wing section

- Only one periodic direction, very small number of pseudo environments for training (162).
- We need to simulate small scales in the leading edge with limit the time step.
- High-fidelity simulation of a wing is computationally expensive (65 million grid points).

Wang, Suárez and Vinuesa (2025)

# DRL control of skin friction in turbulent wings NACA4412 wing at $Re_c=200,000$ , $AoA=5$ deg.



- Use channel flow to train different wing areas (matched  $Re_\theta$ )
  - Increase number of **pseudo environments** from 162 (wing) to 3,240 (channel): Factor of 20 (two periodic directions and big domain).
  - Increase **time step** by a factor of 3 (we do not simulate small scales in the leading edge).
  - Wing has 176 times more points.
  - Training in the channel: 60 times faster and ~10,500 times cheaper.
- Wang, Suárez and Vinuesa (2025)

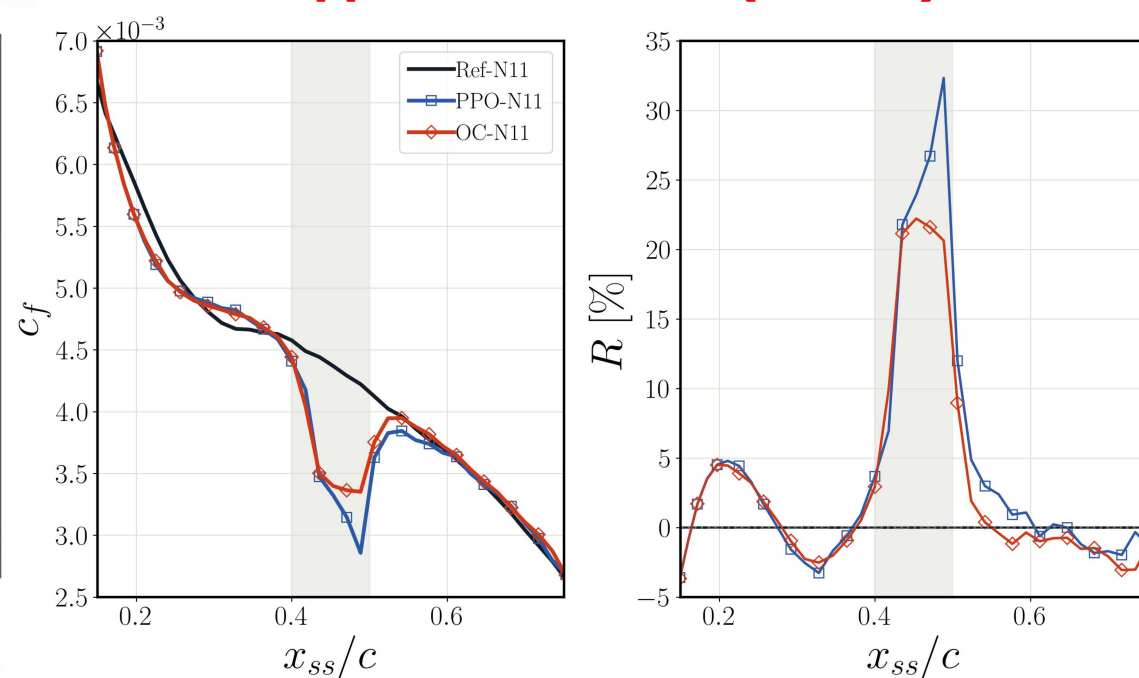
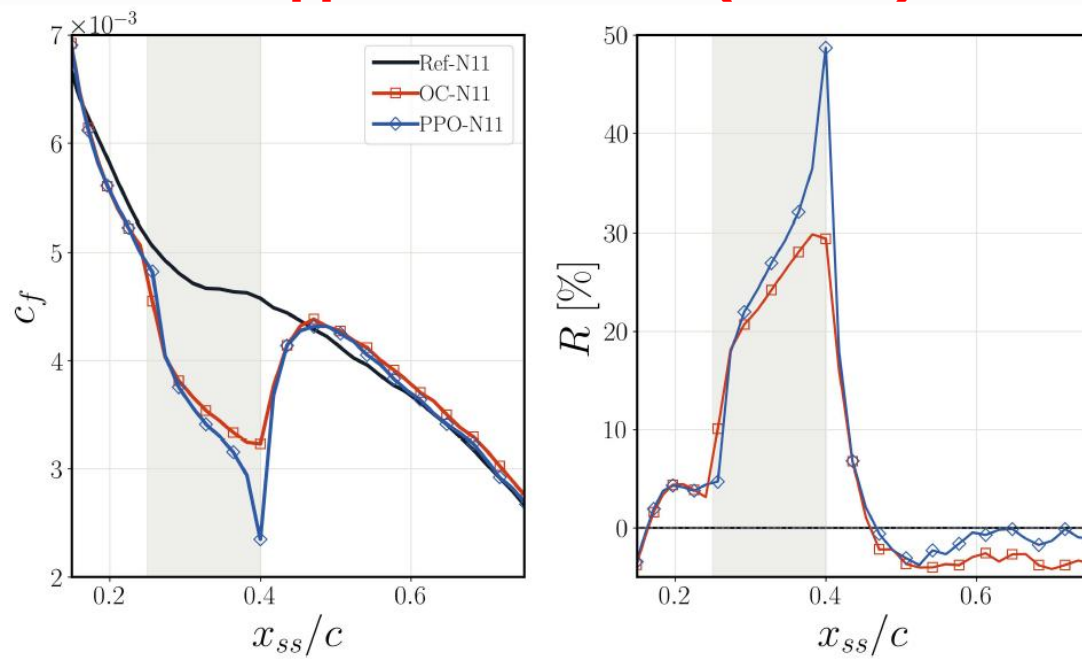


# DRL control of skin friction in turbulent wings NACA4412 wing at $Re_c=200,000$ , $AoA=5$ deg.

- Implementation of control in two regions:  $x/c$  from 0.25 to 0.4 and from 0.4 to 0.5.
- Currently implementing several **simultaneous blocks. DRL 50% better than OC!**

**DRL higher drag reduction (48.7%)** than **opposition control (29.8%)**

**DRL higher drag reduction (32.3%)** than **opposition control (22.2%)**

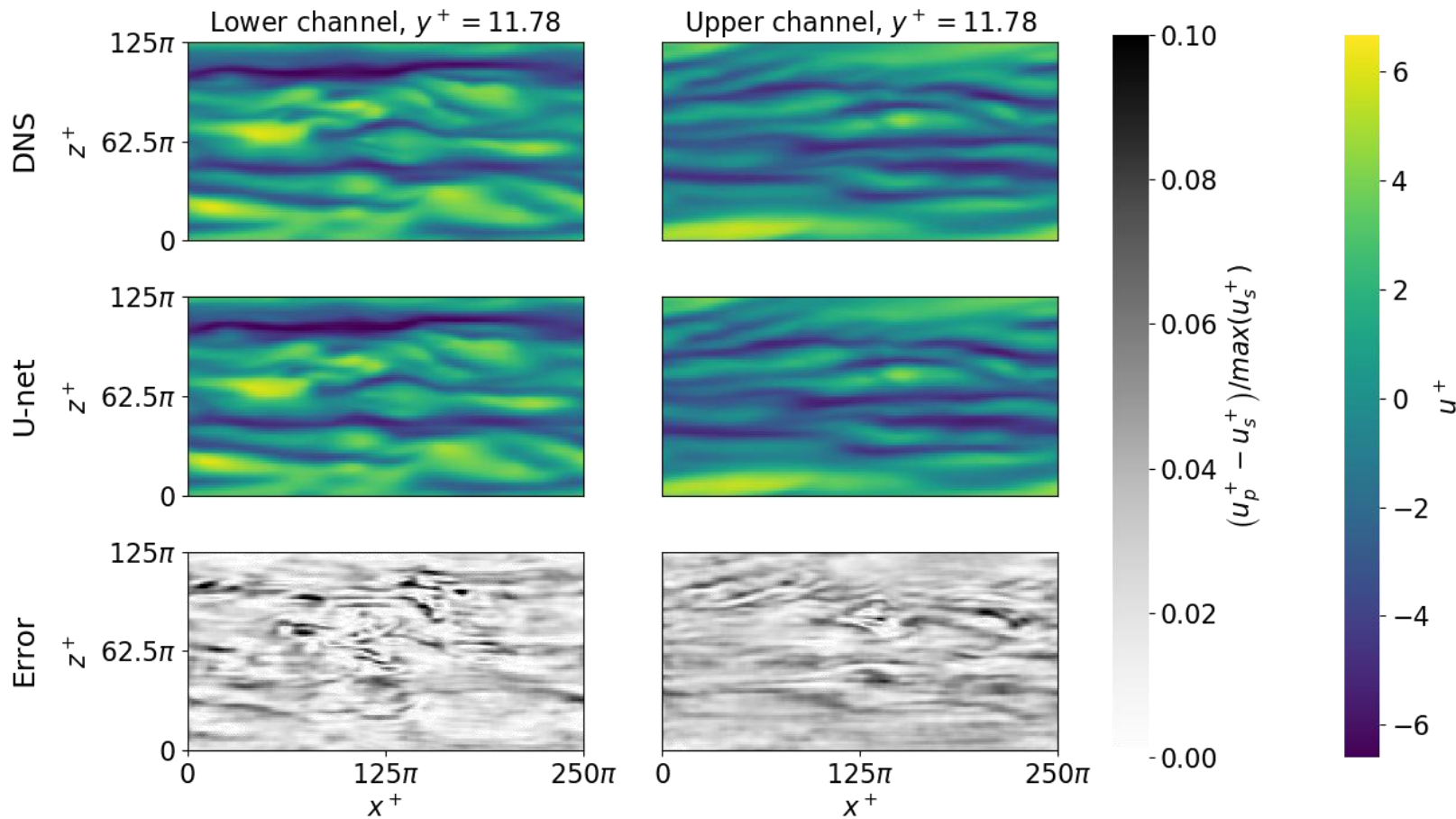


Wang, Suárez and Vinuesa (2025)



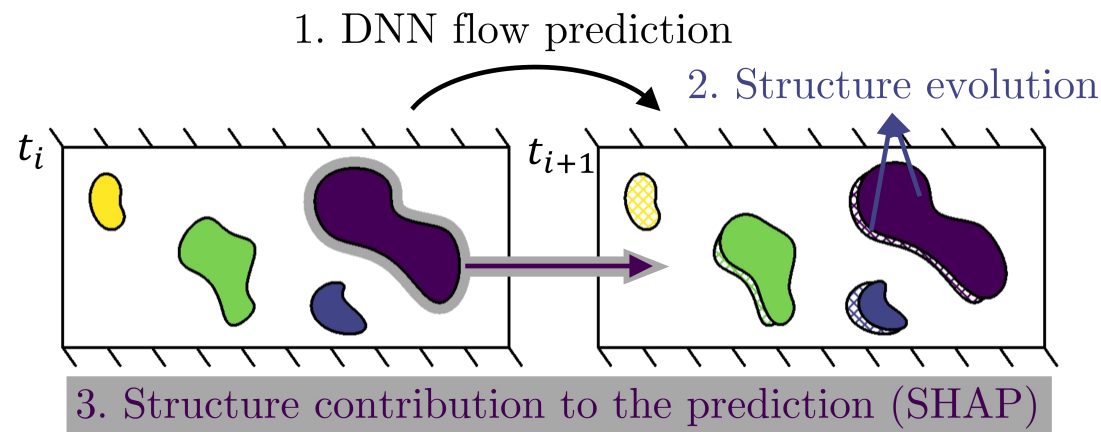
# Prediction results

- Very accurate predictions of the instantaneous velocity fluctuations (periodic padding).
- **Mean relative error is around 2%. Example  $u'$ :**



# The two main assumptions in the kernel-SHAP method

1. **The model  $g$  is linear.** Linear function to represent the error between the predicted and the true fields. In practice, there are so many structures (features), that the **difference** between the true error ( $f$ ) and the linear model ( $g$ ) is **very small:  $(f-g)^2 \sim 10^{-7}$ .**
2. **Contribution of structures to error.** Although the contribution to the error is calculated for 1 structure, and turbulence is highly chaotic, in the kernel-SHAP method the contribution is taken for a number of **coalitions**, which are groups of structures. This accounts for different **inter-structure interactions** when computing the contribution of the structure to the error. **Weighted average of the contribution to the error.**



## Control

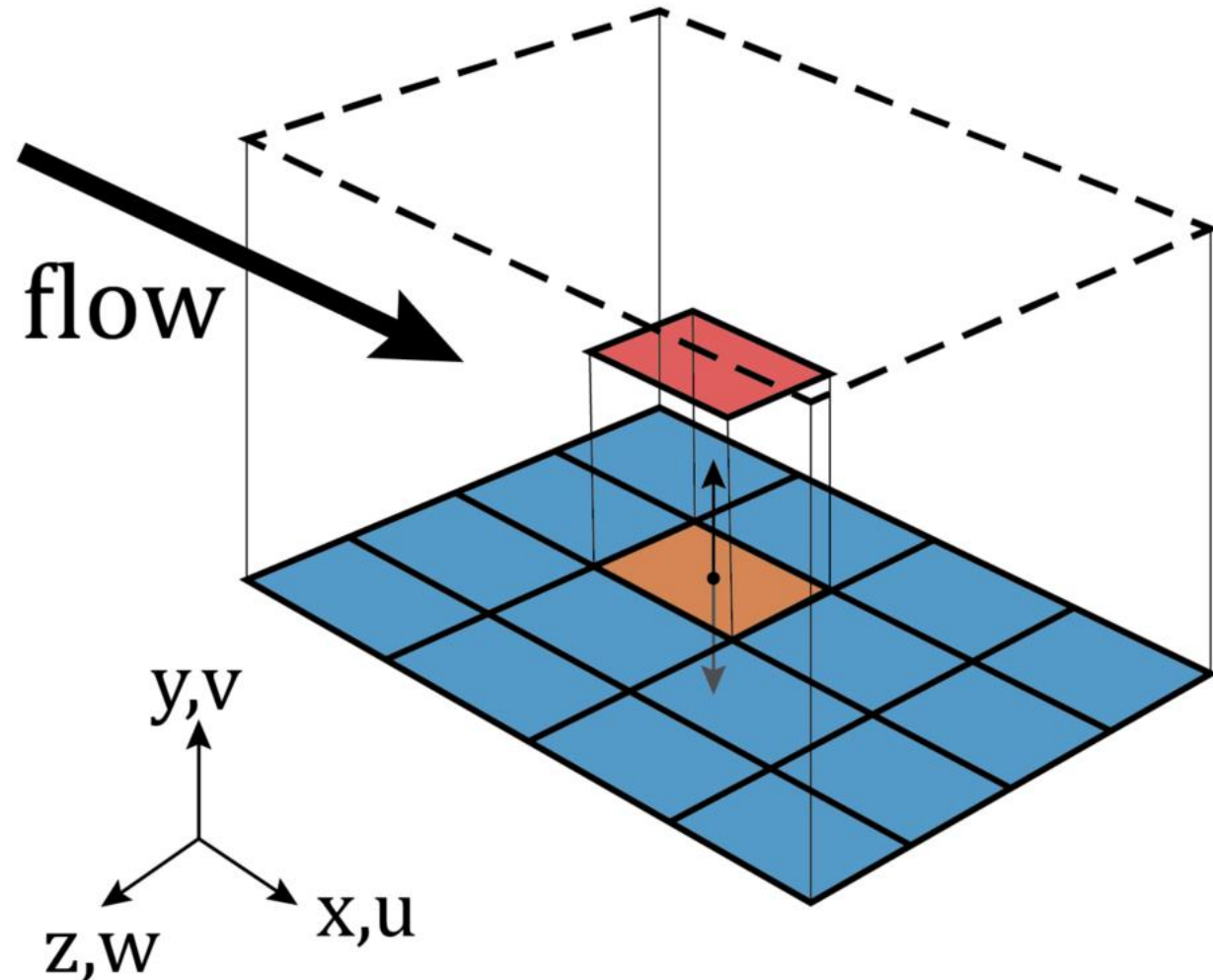
- Actuation interval  $\Delta t^+ \approx 0.6$
- Linear transition from the old value to the new one
- Limited actuation intensity:  $[-u_\tau, u_\tau]$
- All actuators use the same policy:  

$$\pi(s) = \pi(s|\theta)$$

## Policy-learning

- Deep deterministic policy gradient (DDPG)<sup>1</sup> model-free off-policy actor-critic
- Policy gradient update  $\Delta t^+ = 6$
- 64 minibatch gradient-based updates
- 1000 actuations per episode

1. T. P. Lillicrap, J. J. Hunt, A. Pritzel, N. Heess, T. Erez, Y. Tassa, D. Silver, D. Wierstra (2015). Continuous control with deep reinforcement learning, arXiv:1509.02971



# Estimation the cost of the actuation

- How to calculate the net-energy saving?  
Referring to Kametani *et al.*<sup>1</sup>, the input power is:

$$w_{in} = \frac{1}{2} \|v_{wall}\|^3$$

- The net-energy saving will be:

$$S = \frac{c_{f,uncontrolled} - (c_f + w_{in})}{c_{f,uncontrolled}}$$

$\approx 10^{-2}$   
 $\approx 10^{-6}$

- Note that:

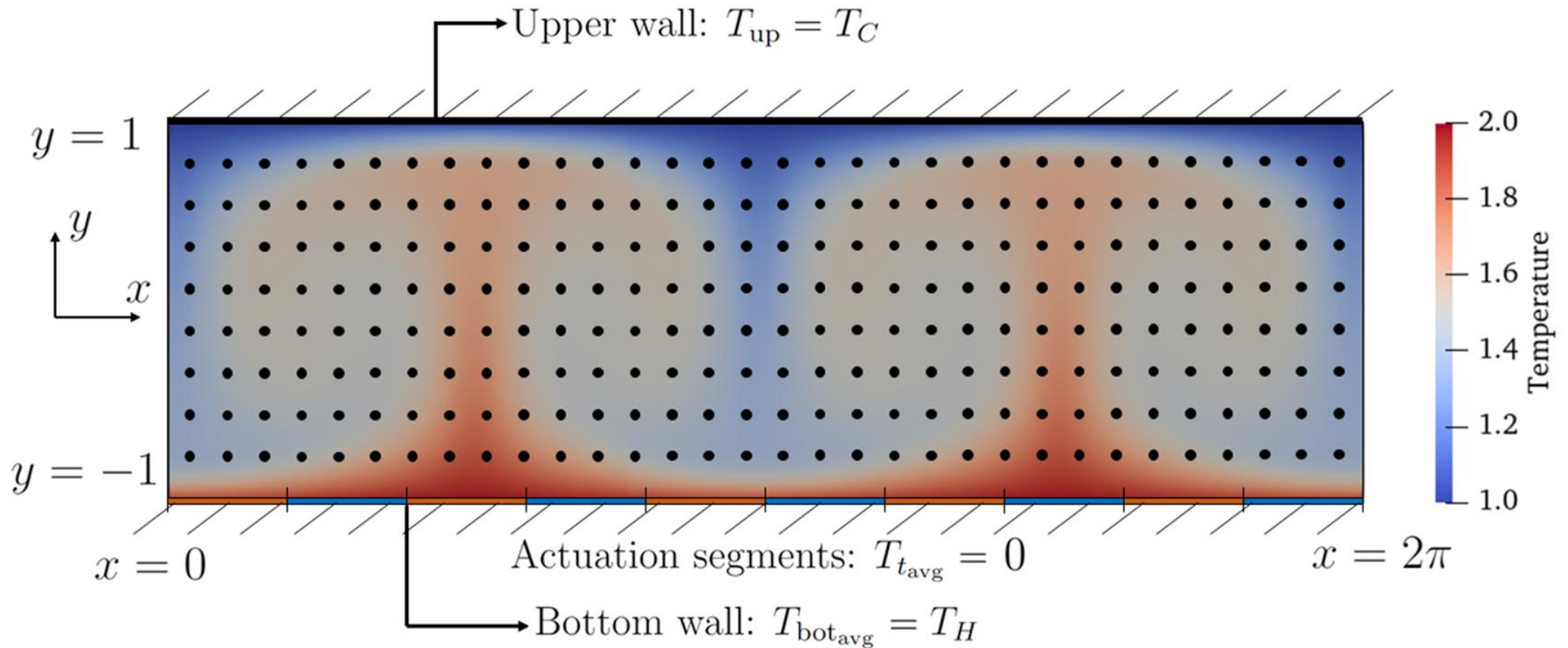
$$R = 1 - c_f / c_{f,uncontrolled} = 1 - \tau_w / \tau_{w,uncontrolled} \approx 10^{-3}$$

- Even if  $w_{in,DRL} > w_{in,Opp}$ , the actuation cost is negligible

# Other applications: Rayleigh–Bénard convection

**Objective:** Reduce Nusselt number, i.e. ratio of convective to conductive heat transfer between two plates (bottom hot, top cold).

- Multi-agent DRL has been successfully applied to Rayleigh-Bénard convection<sup>1</sup>

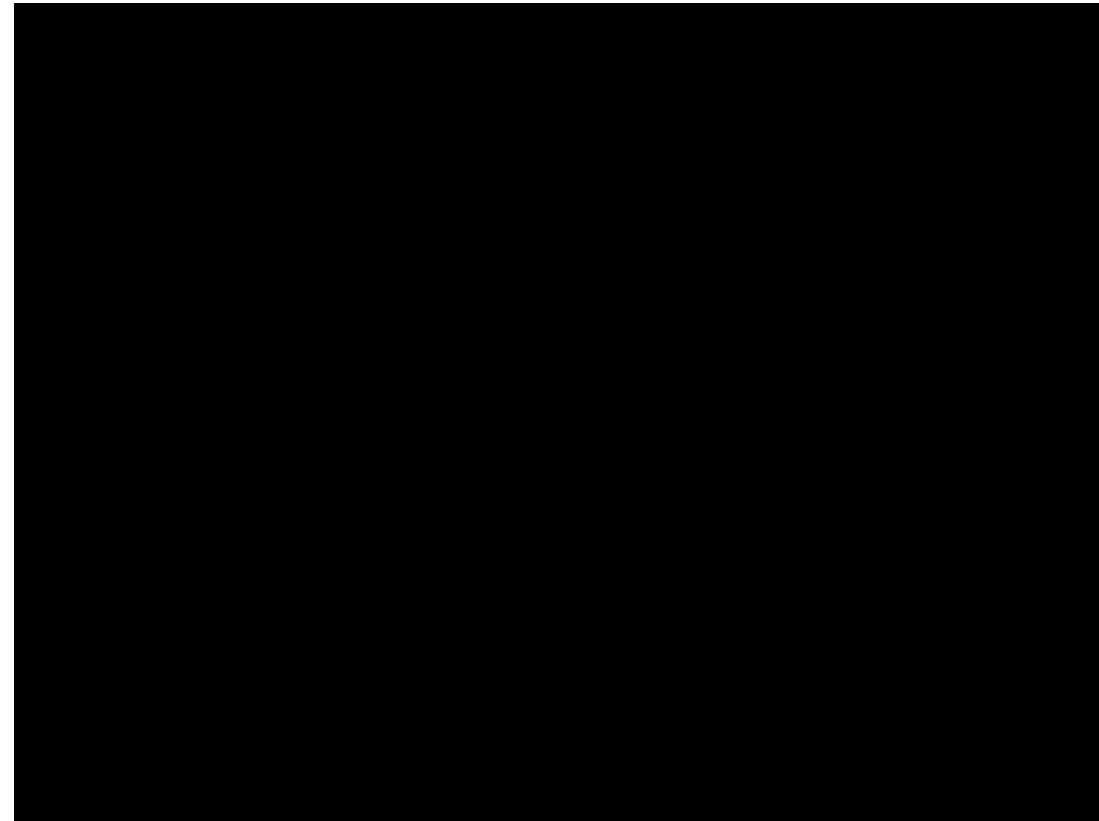
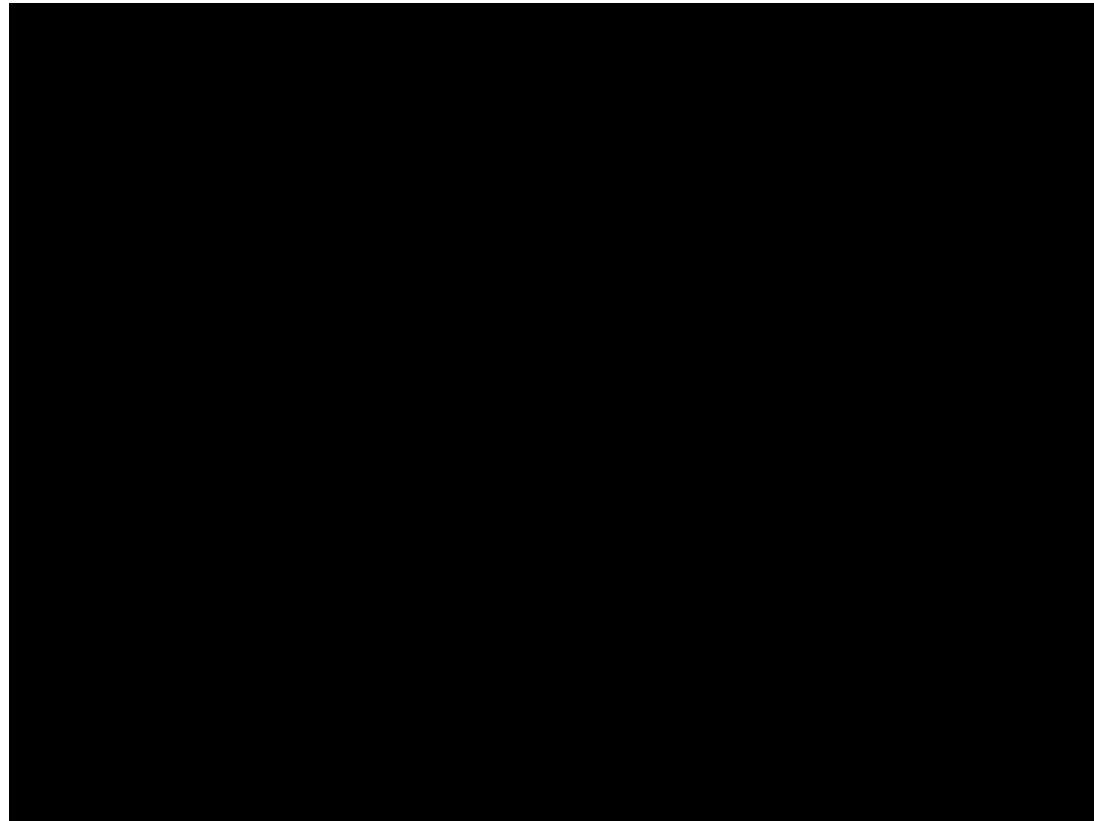




# Single- versus multi-agent reinforcement learning

Single-agent reinforcement learning

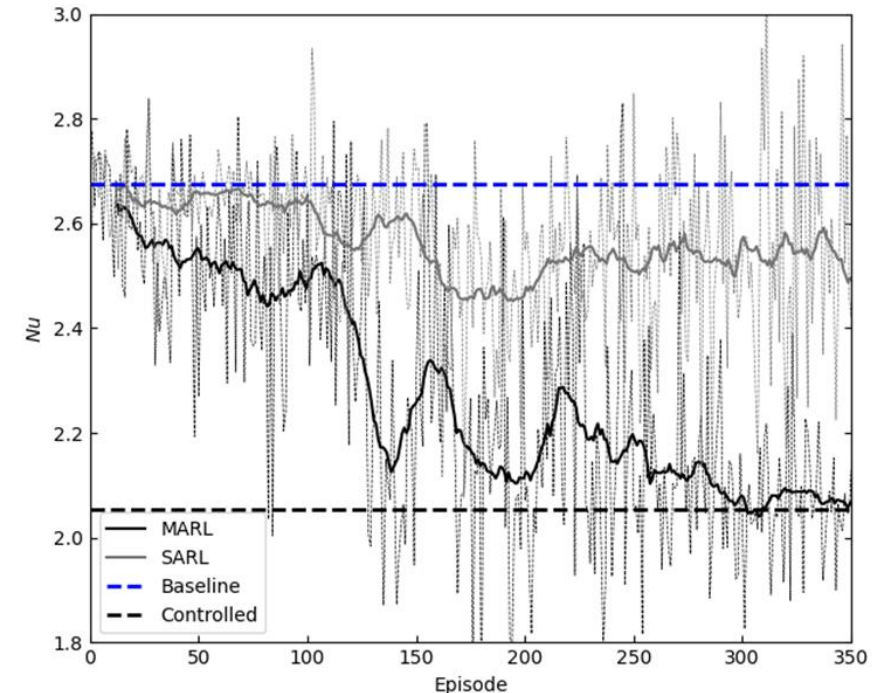
Multi-agent reinforcement learning



Vignon et al., Phys. Fluids 35, 065146 (2023)

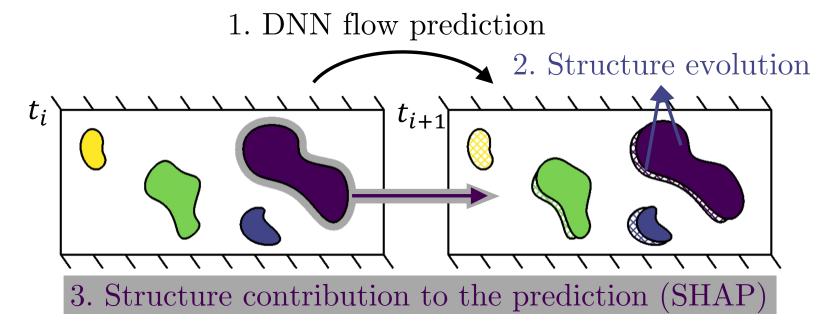
# Other applications: Rayleigh–Bénard convection

- Multi-agent DRL has been successfully applied to Rayleigh–Bénard convection<sup>1</sup>
- The objective is to reduce the Nusselt number  $Nu$ , starting from a given initial condition
- Single-agent RL only offers a limited reduction
- Multi-agent RL provides a more consistent reduction



# The two main assumptions in the kernel-SHAP method

1. **The model  $g$  is linear.** Linear function to represent the error between the predicted and the true fields. In practice, there are so many structures (features), that the **difference** between the true error ( $f$ ) and the linear model ( $g$ ) is **very small:  $(f-g)^2 \sim 10^{-7}$ .**
2. **Contribution of structures to error.** Although the contribution to the error is calculated for 1 structure, and turbulence is highly chaotic, in the kernel-SHAP method the contribution is taken for a number of **coalitions**, which are groups of structures. This accounts for different **inter-structure interactions** when computing the contribution of the structure to the error. **Weighted average of the contribution to the error.**
  - These simplifications are needed to make the problem **computationally feasible.**
  - Typically we have around  $|Q| = 150$  structures per field, yielding **150! Coalitions.**
  - Kernel SHAP randomly selects  $2|Q| + 2048$  coalitions, and the importance of each structure in the coalitions where it is present is **weighted to provide the final SHAP value.** Results shown to converge to the values using more coalitions.





# More details on the kernel-SHAP method

- It is common to use a **linear model** for the error. Note that  $(\mathbf{f}-\mathbf{g})^2 \sim 10^{-7}$  in this work.

Reference output of  $g$  (all structures are absent).

Total number of structures

Presence (1) / Absence (0) of structure 1

$$g(q') = \phi_0 + \sum_{i=1}^N \phi_i q'_i = \phi_0 + \phi_1 q'_1 + \phi_2 q'_2 + \dots + \phi_N q'_N$$

Linear model of error between predicted and true fields

Marginal contribution to error (SHAP value) of structure 1 (negative, structure presence reduces the error)

- We use **kernel SHAP**, which relies on two techniques: **LIME** and **Shapley values**.

- In LIME we formulate the linear optimization problem as follows:

$$\xi = \arg \min_{g \in \mathcal{G}} \mathcal{L}(f, g, \pi_x) + \Omega(g).$$

Local kernel

Loss function

Error between original and ground truth

Penalization of model complexity





# More details on the kernel-SHAP method

- To ensure a unique solution, LIME needs to satisfy several **properties** (local accuracy, consistency, etc.) which are satisfied by the classical **Shapley values**.
- Shapley value: marginal contribution of a particular **structure i (feature)** to the **error f** when included in a particular **group of structures (coalition)**:

$$\phi_i(Q, f) = \sum_{s \subseteq Q \setminus \{i\}} \frac{|s|!(|Q|-|s|-1)!}{|Q|!} (f(s \cup \{i\}) - f(s)),$$

Annotations for the equation:

- Set containing all the structures in a field (points to  $Q$ )
- Total number of structures in the field (points to  $|Q|!$ )
- Total number of possible coalitions not containing  $i$  (points to  $|s|!(|Q|-|s|-1)!$ )
- Coalition without  $i$  (points to  $f(s \cup \{i\}) - f(s)$ )

- Basically evaluates all possible coalitions, identifies all where  $i$  is present, and gets a **weighted average of the contribution of  $i$  to the error  $f$** . **Emulate inter-scale interactions in turbulence.**
- Extremely **challenging from a computational point of view.**

**FLOW**



# More details on the kernel-SHAP method

- Kernel SHAP is an approximation to the Shapley values:

$$\Omega(g) = 0,$$

Mapping from binary space to input space

$$\mathcal{L}(f, g, \pi_x) = \sum_{q' \in Q} [f(h_x(q')) - g(q')]^2 \pi_x(q'),$$

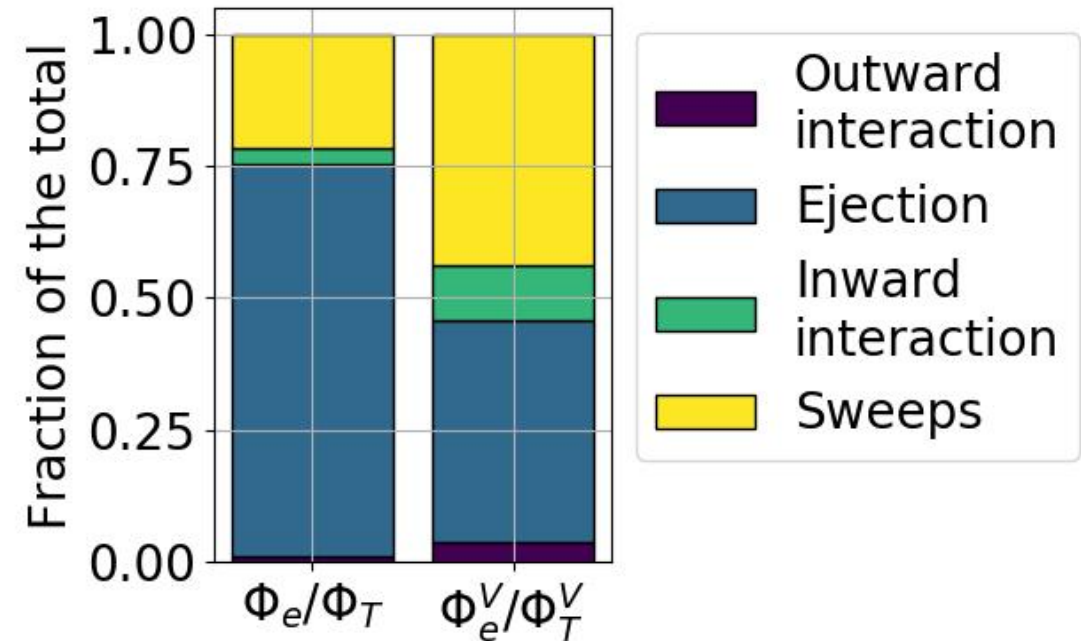
$$\pi_x(q') = \frac{|Q|-1}{\binom{|Q|}{|q'|} |q'|(|Q|-|q'|)}.$$

Number of nonzero structures

- LIME equation solved with linear regression, obtaining  $(\mathbf{f}-\mathbf{g})^2 \sim 10^{-7}$  in this work.
- Typically we have around  $|Q|=150$  structures per field, yielding  $150!$  Coalitions.
- Kernel SHAP randomly selects  $2|Q|+2048$  coalitions, and the importance of each structure in the coalitions where it is present is weighted to provide the final SHAP value.

# Importance of the various structures

- Higher SHAP absolute value (+ o -) implies higher importance.
- ~60% of the structures are sweeps or ejections.
- 97% of the SHAP is from ejections (75%) and sweeps (22%).
- Importance per unit volume: **ejections 42%** and **sweeps 44%**.





# Reinforcement learning terminology

- **Model-based RL:** Use transition probability distribution and reward function (**model of the environment**) from the **Markov decision process**.
- **Model-free RL:** Does **not use them, explicit trial and error**.
  - **Q learning:** We try to **learn everything about the system**, and how the reward changes for given actions. Q estimates the reward, assigning a value of reward to any given action for a particular state.
  - **Policy-gradient methods:** We **do not learn everything** about the system, but rather how to **maximize the reward**. Relies on a stochastic policy  $\pi$  (distribution for each state input) parametrized by a NN.
  - **Deep deterministic policy gradient (DDPG):** Combines aspects **of Q learning and policy gradient**. Does not differentiate positive and negative actions, use **actor-critic**:
    - **Actor approximates policy**  $\pi$ , which is considered deterministically.
    - **Critic computes Q** function to assess the **goodness** of those actions.
    - **Action space** is **explored** via a perturbative method through **noisy processes**.

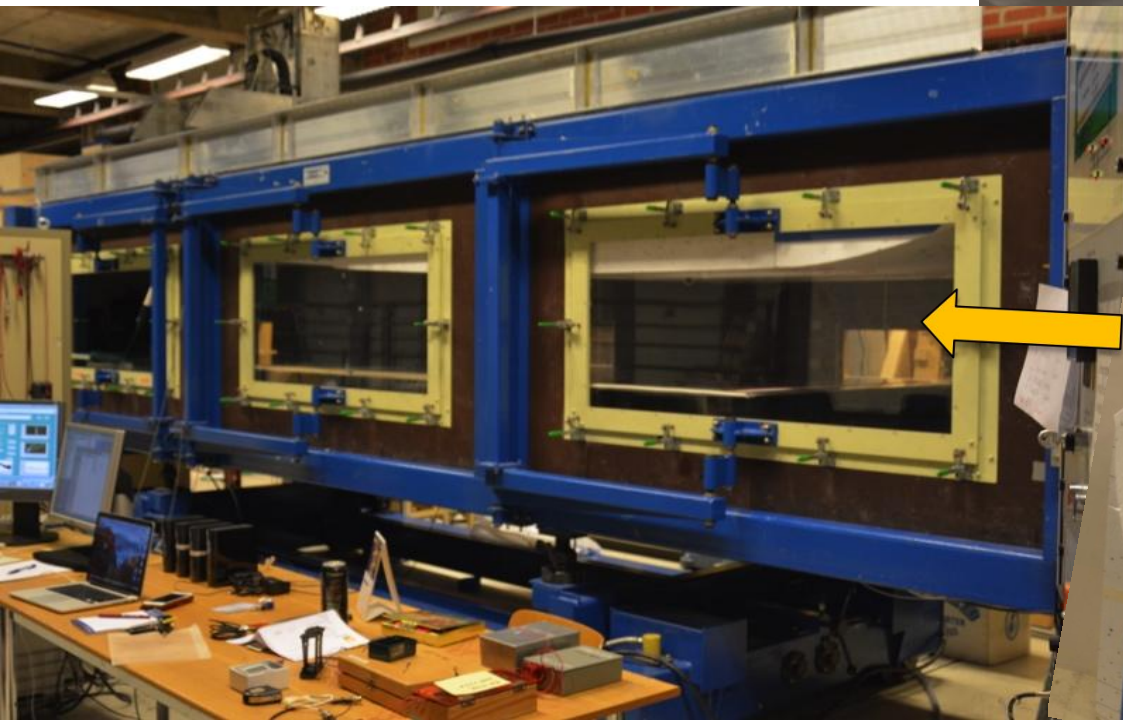
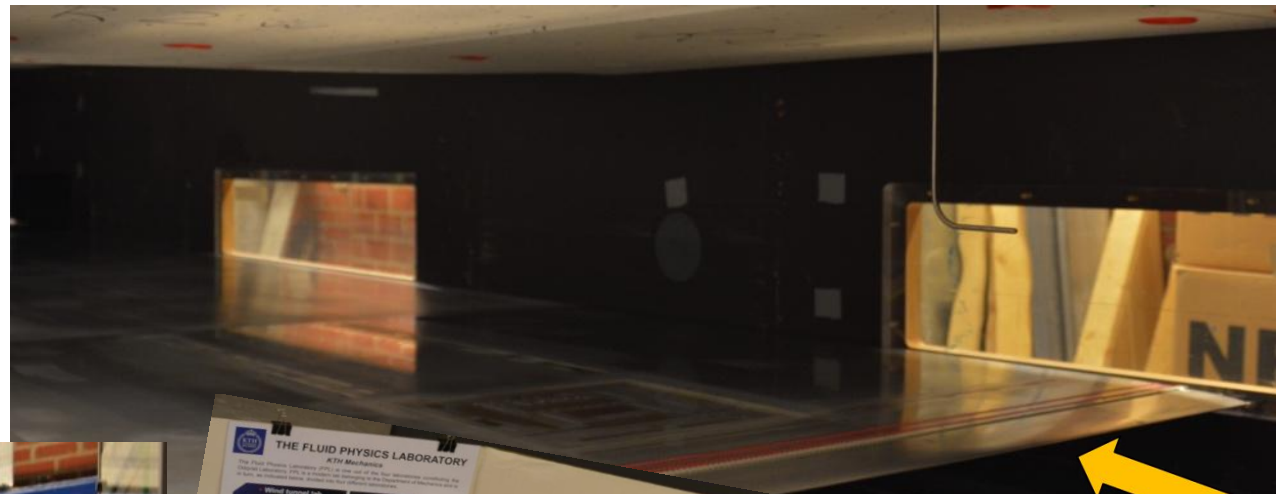


# Flat-plate APG TBLs: (MTL) wind-tunnel experiments and simulations

Both to match the LES conditions in  $Re$  and  $\beta$  as well as further extend the  $Re$  range. Mainly HWA measurements, incl. planar PIV with different resolutions and OFI.

## Styrofoam roof inserts for PG.

Sanmiguel Vila et al. Phys. Rev. Fluids 5 (2020)





# Comparisons at matched parameters: $Re_{\tau} \approx 4500$ & $\beta \approx 1.2$

Sanmiguel Vila et al. Phys. Rev. Fluids 5 (2020)

